Study of composite-aluminum hybrid crash absorbing components.

Bachelor Thesis

Eric Escobar Ortiz-Villajos

Tutor : Carlos Santiuste Romero

Grado en Ingeniería Aeroespacial

Escuela Politécnica superior

Departamento de Mecánica de Medios Continuos y Teoría de Estructuras.

Annex

Este proyecto ha sido apoyado por Airbus mediante una beca de colaboración.

Departamento de Dinámica Estructural y Aeroelasticidad

Tutor en Airbus: Héctor Climent Mañez

Tutor en Airbus: Juan Tomás Viana Lozoya

Table of Contents

Page

List of Tables **iii**

List of Figures **iv**

1 Introduction **1**

1.1 Motivation 1

1.1.1 Basics 1

1.1.2 Historical development 2

1.1.3 Industry application 3

1.2 Goals 6

1.3 Project Plan 7

2 Background **8**

2.1 Typical Absorption Energy Structures 8

2.1.1 Concept 8

2.1.2 Crashing components 9

2.2 Composite Materials 10

2.3 Finite element analysis 14

2.3.1 Introduction 14

2.3.2 Finite Element Analysis concept 14

2.3.3 Element definition 17

2.3.4 Solving method. Implicit vs explicit: 18

3 3. Axial Beam Crushing **20**

3.1 Test Description 20

3.2 Model Description 23

3.2.1 Geometry 23

3.2.2 Mesh . . . 24
3.2.3 Material properties: . . . 28
3.2.4 Boundary and initial conditions scheme . . . 30

4 Aluminum crushing beam study. Model results 36
4.1 First Approximation . . . 36
4.2 Softwares Analysis . . . 37
4.3 Solid Aluminum Abaqus . . . 37
4.4 Shell Aluminum Abaqus . . . 38
4.5 Solid Aluminum Pam-Crash . . . 40
4.6 Shell Aluminum Pam-Crash . . . 41
4.7 Results Comparison . . . 42
4.7.1 Abaqus vs Pam-Crash . . . 44

5 Hybrid crushing beam study 45
5.1 Pam-Crash Hybrid model . . . 45
5.2 Abaqus Hybrid model . . . 47
5.2.1 Hybrid model for $[0°]_2$: . . . 47
5.2.2 Hybrid model for $[90°]_2$: . . . 49
5.2.3 Hybrid model for $[+45°/-45°]_2$: . . . 50
5.2.4 Hybrid model for $[90°/0°]_2$: . . . 51
5.3 Results Comparison . . . 52

6 Conclusions, Applications and Future "To-do's" 54
6.1 Conclusions . . . 54
6.2 Applications - Weight Saving of Hybrid Structure. . . . 55
6.3 Future works: . . . 57

7 ANNEX - Budget 58

Bibliography 59

List of Tables

Table **Page**

4.1 Comparison of the Energy Absorbed for the Aluminum bar 42
4.2 Pam-Crash vs Abaqus. Computational data comparison. 43

5.1 Hybrid beam. Energy absorption depending on ply orientation. 52
5.2 Hybrid beam. Maximum Displacement (δ_{max}) depending on ply orientation. . 52

List of Figures

Figure **Page**

1.1 Evolution of airliners casualties.[16] . . . 3
1.2 Automobile fuselage. Crash box beams . . . 4
1.3 Audi's bumper. Axially tested . . . 4

2.1 Scheme of a cantilever beam . . . 8
2.2 Angular loading effects [4] . . . 9
2.3 A320 fuselage . . . 10
2.4 Composite lay-up . . . 10
2.5 Rear BMW i3 bumper . . . 11
2.6 Composite loading direction scheme . . . 12
2.7 Complex part divided in tiny elements . . . 15
2.8 Solid to shell simplification . . . 17
2.9 Solid formulation scheme . . . 18

3.1 Test arrangement . . . 21
3.2 Aluminum collapse sequence . . . 21
3.3 Force vs Displacement for Aluminum . . . 22
3.4 Force vs Displacement for Hybrid structure for [0°] degrees ply . . . 22
3.5 Hybrid structure for [0°] degrees plies . . . 23
3.6 Whole model assembly . . . 23
3.7 Mesh convergence . . . 24
3.8 Mesh for Aluminum beam . . . 25
3.9 Aluminum partition needed for mesh . . . 26
3.10 Impactor plate mesh . . . 26
3.11 Reduced Aluminum Mesh . . . 27
3.12 Outer composite Mesh . . . 27
3.13 Stress-Strain curve for Al 6063T5 . . . 28

3.14 b.c and i.c display 30
3.15 Paris Law 31
3.16 a)Beam arrangement b)Aluminum beam after impact 32
3.17 Undistorted beam - No buckling 33
3.18 Spurious mode. Views 1 and 2 34
3.19 Distortion needed for lobes formation 34

4.1 Undistorted beam - No buckling 36
4.2 Aluminum Collapse Sequence. Test vs Simulation 37
4.3 Force vs Time. Abaqus Solid 38
4.4 Deformed aluminum. Abaqus Shell 38
4.5 Force vs Time. Abaqus Shell 39
4.6 Deformed beam. Pam-Crash solid 40
4.7 Force vs Time. Pam-Crash Solid 40
4.8 Deformed beam. Pam-Crash Shell 41
4.9 Force vs Time. Pam-Crash Shell 41
4.10 Force vs displacement comparison. Test vs Simulations 42

5.1 Pam-Crash hybrid beam for [0°] degrees plies 46
5.2 Puck equation[11].Outside of the parabola failure will occur. 46
5.3 Abaqus hybrid beam for [0°] plies. Simpler Mesh 47
5.4 Abaqus hybrid beam for [0°] plies. Complex Mesh 47
5.5 Force vs Displacement. Test vs Simulation comparison 48
5.6 Force vs Displacement. Test vs Simulation comparison 48
5.7 Abaqus hybrid beam for [90°] plies. Coarse Mesh 49
5.8 Force vs Displacement. Test vs Simulation comparison 49
5.9 Abaqus hybrid beam for $[+45°/-45°]$ plies. Coarse Mesh 50
5.10 Force vs Displacement. Test vs Simulation comparison 50
5.11 Abaqus hybrid beam for [90°/0°] plies. Coarse Mesh 51
5.12 Force vs Displacement. Test vs Simulation comparison 51

6.1 Different beam arrangement comparisons 55
6.2 A320 fuselage model.Free fall tested 56

CHAPTER 1

INTRODUCTION

1.1 Motivation

1.1.1 Basics

On average more than 32.000 people die per year involved in crash accidents only in the US. It is estimated that since the development of the automotive industry, more than 3.5 million people have lost their lives in car accidents in the US. Even though in this industry is where most lives are lost every year it is not the only one. In the aeronautical industry any crash will end up most likely with the loss of the whole crew. This is why it is crucial to investigate into this topic so that if an accident occurs the casualties can be minimized.

Crashworthiness is the ability of a structure to protect its occupants during an impact. It is a common test for any means of transport safety. Depending on the characteristics of the impact and the vehicle involved, different criteria are used to assess the crashworthiness of the structure. Crashworthiness may be predicted using finite element models (e.g., Abaqus, Pam-Crash, LS-DYNA) or experiments. It can also be studied by analyzing crash outcomes. In the aeronautical field, every time there is a fatal crash, this investigation is conducted. Several criteria are used to assess crashworthiness such as deformation patterns of the vehicle structure, the acceleration experienced by the vehicle during an impact, the energy absorbed by the structure and the predicted probability of

injury. [18]

Typical crushing characteristics are non-linearity of the impact, usually relatively high velocities (even though a large mass moving at a lower velocity -same energy- can also simulate the same experiment) and the predominance of plasticity.
The objective of crashworthiness is to design a structure that in case of a hazardous situation is able to absorb the energy of an impact trying to minimize the damage sustained by the rest of the structure (fail safe design) so that the human damage can be avoided. The ideal crash absorber would end up completely destroyed while protecting the rest of the structure from damages.

1.1.2 Historical development

"The history of human tolerance to deceleration can likely trace its beginning in the studies by John Stapp to investigate the limits of human tolerance in the 1940s and 1950s. In the 1950s and 1960s, the US Army had serious accident related to crashworthiness as a result of fixed-wing and rotary-wing accidents as helicopters became the primary mode of transportation in Vietnam. Pilots were receiving spinal injuries in otherwise survivable crashes due to decelerative forces. The investigation started to develop energy absorbing seats to reduce the chance of spinal injuries during training and combat. Heavy research was conducted into human tolerance, energy attenuation and structural designs that would protect the occupants of military helicopters. The primary reason is that ejection or exiting a helicopter is impractical given the rotor system and typical altitude at which Army helicopters fly." [15]

Regarding to the aeronautical field, its safety has always been one of the main concerns stopping people from using it. Nevertheless, as it can be seen in picture 1.1 deaths caused by airliners are far below those of other means of transport.

With respect to automotive crashworthiness some of the main milestones are dated as follows:

-In 1922, first car to have four-wheel hydraulic brakes.
-In 1930, safety glass became standard on all Ford cars.

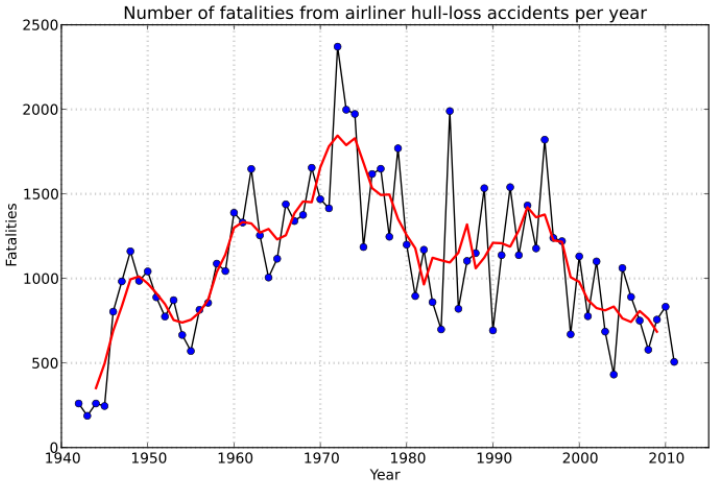

Figure 1.1: Evolution of airliners casualties.[16]

-In the 1930s, seat belts started to be used.
-In 1934, first crash test was performed.
-In 1936, first back-up brake system.
-In 1949 SAAB incorporated aircraft safety thinking into automobiles making the Saab 92 the first production SAAB car with a safety cage.

Crashworthiness was greatly improved in the 1970s with the fielding of the Black Hawk and the Boeing AH-64 Apache helicopters. Primary crash injuries were reduced, but secondary injuries within the cockpit continued to occur. This led to the consideration of additional protective devices such as airbags. Airbags were considered a viable solution to reducing the incidents of head strikes in the cockpit, and were incorporated in Army helicopters. [17]

As it usually happens, the research conducted in the aeronautical sector ended being useful for other industries such as the automotive. Airbags and energy absorbing seats are nowadays installed in every car.

1.1.3 Industry application

There is a distinction between aeronautical and automotive crashworthiness, in the aeronautical the aim is usually to abandon the ship. However, there are no ejection

mechanisms for automobiles. This is why in automobiles the main crash absorbing structure is in the front part, the bumper. The bumper is the primary crash absorbing structure while the airbags or energy absorbing seats are secondary devices. In a car the structure design to sustain the crushing loads is the crash box, which consist on two beams located immediately behind the bumper. The bumper is usually a beam made of metal. In the late 80's these bumpers were made of steel until the superior specific properties of Aluminum were discovered and exploited. Aluminum is better for this purpose because being a soft material allows it to deform greatly absorbing more energy than steel. An Aluminum crash box can be seen in figure 1.2

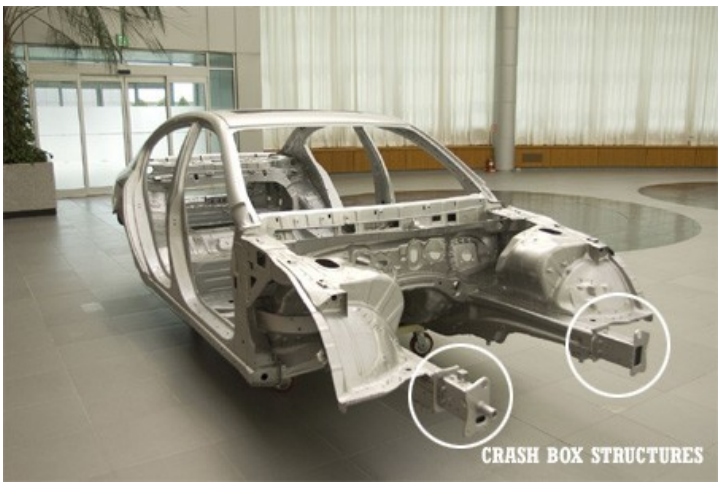

Figure 1.2: Automobile fuselage. Crash box beams

Knowing beforehand how the material will deform or how it should deform so that the maximum energy can be absorbed is crucial to a proper design. The following picture 1.3 is a crash box tested by Audi.

Figure 1.3: Audi's bumper. Axially tested

The most remarkable thing about the figure 1.3 is the large number of lobes formed. With this crushing pattern the structure is able to maximize the energy absorption.
Once the metal structure has given its maximum, in this case the aluminum, the following step is to mix it with other materials aiming to combine properties. This can be done in several manners. The aluminum can be filled with materials such as wood, or foams so that when it tries to buckle in, the filling part has to be deformed achieving further energy absorption. A different way to do this but based on the same idea is to cover the metal with composite layers so that when the lobes try to form, the composite opposes to this movement allowing once again for a greater energy absorption.

In this project the aluminum beam was covered with composite materials since it is an approach that has been very little studied. Composites materials on their own are not reliable energy absorbers since they are very brittle and prone to failures such as delamination and crack propagation. However, an hybrid structure in which every material works in the way it is known to work better and can exhibit properties much better than each of the materials working separately.

1.2 Goals

The purpose of this Bachelor's project is to understand the crushing behavior of hybrid components which is quite a new field and has not been researched enough. As composites are increasing exponentially their presence in almost every industry, the understanding of their crashing behavior is crucial to save people's lives.

For doing so it is aimed to reproduce the test results obtained by Hee Chul Kim, Dong Kil Shin, Jung Ju Lee and Jun Beom Kwon [2]. In their work, they test the crashworthiness capabilities of an aluminum beam. The aluminum beam is then covered with composite layers in different orientations. Comparing the energy absorption and how much the structure deforms for different plies orientation, they were able to assess which plies stacking and orientations are best.

This cross-check will be done with finite element softwares. Two different softwares for Finite Element Analysis are used, Abaqus and Pam-Crash. Results between softwares and the real experiment will be compared. Apart from double-checking results, the use of different softwares allows to compare interesting parameters amongst them such as the time-step, calculation times and outputs files sizes.

Once the model is validated, it is intended to suggest extra orientations different from those tested.

1.3 Project Plan

Before starting to work with the Finite Element Model reproduction, research was conducted in necessary fields to have a proper understanding of the project. This includes general composite material theory and a basis on finite element analysis.

The paper [2] explaining the test details and results was thoroughly read and understood so that a proper reproduction of the test could be done.

Once the test was understood, it was modeled with the different softwares.

The problem was first solved only for the aluminum beam so that it could be assessed if the results were meaningful before moving to the complex problem.

The aluminum beam was modeled with two different material definitions (shell and solid) which allows for an extra cross-check of results and adds certainty about them.

Once the aluminum beam model is tested its results are be compared with those of the test from the Korean University. It is then decided if a model should be abandoned.

Finally the finite element method composite model is tested. Comparisons for each ply orientation are done between the software and the real test.

A global overview of the project will be then given and all the results will be commented.

CHAPTER 2

BACKGROUND

2.1 Typical Absorption Energy Structures

2.1.1 Concept

The dissipation of energy while undergoing plastic deformation is paramount in relation with the safety of vehicles of all sorts. There is energy absorption as long that there is deformation of a structure. This deformation may be permanent or not. When the deformation is permanent is because plastic deformation has been produced and energy has been absorbed. However, energy can also be stored and when the impactor stops exerting a force, the impacted body will release this energy. In a complex crash structure there is a combination of both behaviors, which are difficult to predict.

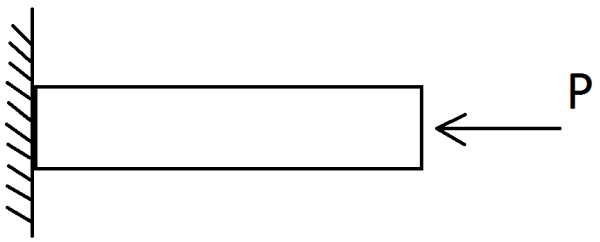

Figure 2.1: Scheme of a cantilever beam

2.1.2 Crashing components

The simpler component regarding energy absorption is a metal beam. This structural element is integrated in more complex structures such as crash bumpers or plane fuselages. The best element for axial crushing is a closed square beam as it was shown by Kim SB in [3]. Open sections are quite unreliable for crashing since the bend really fast, which reduces the load carrying capability. Regarding to closed sections, a square section has been proven to be the best since other sections trigger local bucking. The loading direction is also a very important parameter since any asymmetry in the loading also triggers local buckling that bends the structure reducing its crushing capability significantly.

Figure 2.2: Angular loading effects [4]

In this project purely axial bucking will be considered.

Structures in which it is integrated:
-In the automotive industry this is integrated in the crash-box.
-In the aerospace industry there many parts in which crashworthiness is tested: i.e. lifting surfaces, leading edges or fuselage's nose are tested for bird strikes. The axial crushing beams concept is used in the fuselage beams that support the passenger cabin floor.

The latter example can be seen in the following pictures which correspond to the Airbus A320 free fall test, as seen in figure 2.3.

The elements sustaining the floor are precisely beams working under axial compression.

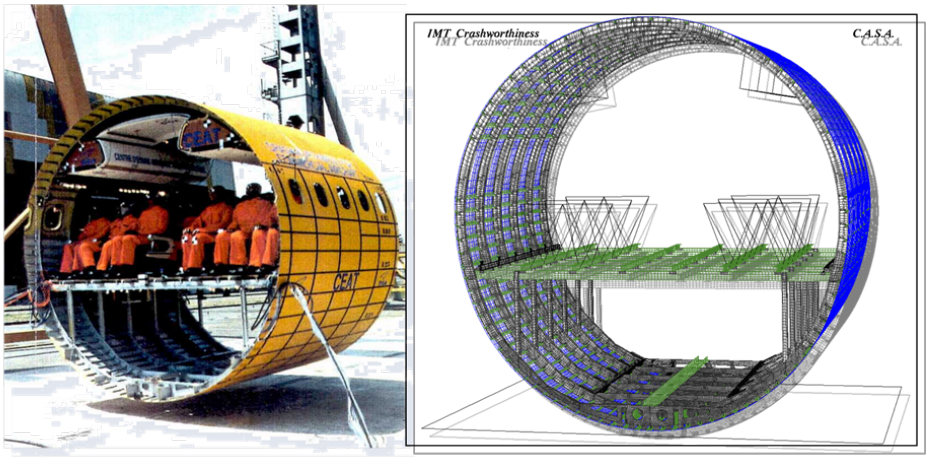

Figure 2.3: A320 fuselage

2.2 Composite Materials

Composites are materials made from two or more materials with significant different properties. When combined, they produce a material whose characteristics are really different from the components. The individual components remain separate and distinct within the structure (the are not melt up together like alloys). The new material can exhibit better properties such as increased yield stress.

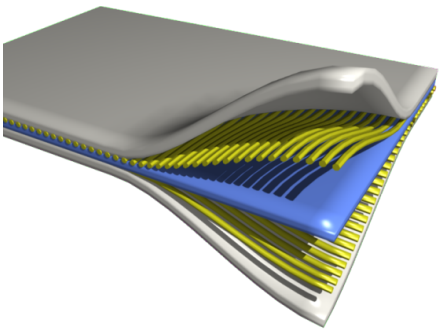

Figure 2.4: Composite lay-up

Typical composites include:
-Composite building materials (concrete or cement)
-Reinforced plastics (CFRP, GFRP)
-Metal composites.

The typical ones for covering a structure, as is being approached in this project, are the laminates which are used in the aeronautical or space field as outer fuselage or skin and also in the automotive industry, e.g. in the F1 cars.
Composite laminates are assemblies of layers of composite fibers joined to provide superior properties. Each layer consist on a fiber which is the element that will influence the most since is the one which properties are aimed to be best and the matrix. The matrix is the element that glue or fix everything together. In this project Carbon Fiber Reinforced Polymer (CFRP) is being used. For this laminate, the matrix or the binding polymer typically consist on a thermoset such as epoxy and the fibers consist on carbon fiber.
Some data regarding carbon fiber, the Airbus A350 is 53% built of CFRP and the Boeing 787 Dreamliner 50%. In the automotive industry we can also find this materials in demanding fields or high quality brands. For example the rear bumper of the BMW i3 is made from a honeycomb of CFRP.

Figure 2.5: Rear BMW i3 bumper

One of the most important properties to take into account when working with composite materials is that their properties are dependent of the fibers direction (orthotropic materials) as it can be seen in figure 2.6.
In the loading direction A (the fiber direction), the load is shared by the matrix and the fibers. Even though it is the fibers the one which carry most of the loads, the matrix contribution is not negligible. On the other hand, in the opposite direction (B), the fibers do not contribute at all to the load carrying capability and its the matrix the one working alone. Fiber are even detrimental for this loading orientation since they are holes in the loading direction.
Composite material properties are therefore needed to be expressed in every loading

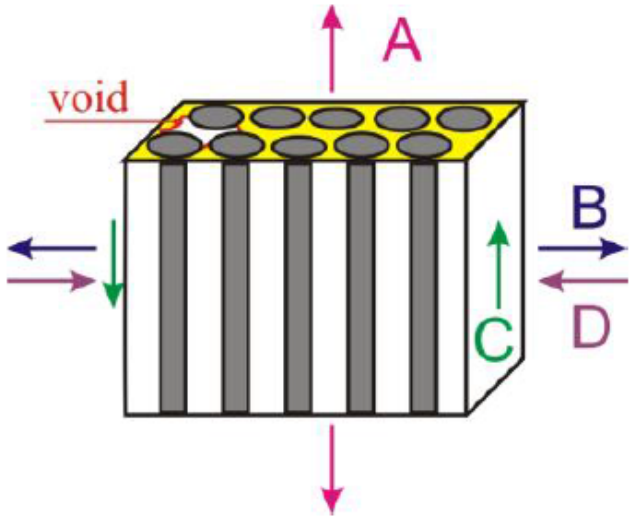

Figure 2.6: Composite loading direction scheme

direction. E, the Young modulus has to be expressed for the fibers direction (E_{12}) for the matrix direction (E_{13}) and for the out of plane loading (E_{23}). And also the Shear Strength, G. Composite material properties can be expressed combined as a whole (the contribution of fiber + matrix working together) or separately for each component. The one used in the project is the one working as a whole.
Composites exhibit failure modes which are exclusive of them such as delamination (separation or debonding of different layers of fibers). Another particularity with composite materials is how the damage evolution is treated since the fibers and the matrix do not work the same if loaded with tension or compression. Fibers are commonly more resistant to tension than compression (usually the double) while the matrix works better in compression than in tension, which tear it to pieces.

As a result of this complex behavior there are many formulations regarding damage evolution of composite materials. In this project the Hashin's Failure Criteria for Unidirectional Fiber Composites was used.

Hashin failure criteria [5] :

This failure criteria considers more than one stress components used to evaluate the different failure modes. These criteria were originally developed for unidirectional polymeric composites, and hence, applications to other type of laminates and non-polymeric

composites have significant approximations. Usually Hashin criteria are implemented within two dimensional classical lamination approach for point stress calculations with ply discounting as the material degradation model. Failure indexes for Hashin criteria are related to fiber and matrix failures and involve four failure modes. The criteria are extended to three dimensional problems where the maximum stress criteria are used for transverse normal stress component.
The failure modes included in Hashin's criteria are as follows.

1. Tensile fiber failure for $\sigma_{11} \geq 0$

$$\left(\frac{\sigma_{11}}{X_T}\right)^2 + \left(\frac{\sigma_{12}^2 + \sigma_{13}^2}{S_{12}^2}\right) = \begin{cases} \geq 1 \; failure \\ < 1 \; no \; failure \end{cases} \tag{2.1}$$

2. Compressive fiber failure for $\sigma_{11} < 0$

$$\left(\frac{\sigma_{11}}{X_C})^2\right) = \begin{cases} \geq 1 \; failure \\ < 1 \; no \; failure \end{cases} \tag{2.2}$$

3. Tensile matrix failure for $\sigma_{11} + \sigma_{22} > 0$

$$\frac{(\sigma_{22} + \sigma_{33})^2}{Y_T^2} + \left(\frac{\sigma_{23}^2 - \sigma_{22}\sigma_{33}}{S_{23}^2}\right) + \left(\frac{\sigma_{12}^2 + \sigma_{13}^2}{S_{12}^2}\right) = \begin{cases} \geq 1 \; failure \\ < 1 \; no \; failure \end{cases} \tag{2.3}$$

4. Compressive matrix failure for $\sigma_{22} + \sigma_{33} < 0$

$$\left[\left(\frac{Y_C}{2S_{23}}\right)^2 - 1\right]\left(\frac{\sigma_{22} + \sigma_{33}}{Y_C}\right) + \frac{(\sigma_{22} + \sigma_{33})^2}{4S_{23}^2} + \frac{\sigma_{23}^2 + \sigma_{22}\sigma_{33}}{S_{23}^2} + \frac{\sigma_{12}^2 + \sigma_{13}^2}{S_{12}^2} = \begin{cases} \geq 1 \; failure \\ < 1 \; no \; failure \end{cases} \tag{2.4}$$

5. Interlaminar tensile failure for $\sigma_{33} > 0$

$$\left(\frac{\sigma_{33}}{Z_T^2}\right)^2 = \begin{cases} \geq 1 \; failure \\ < 1 \; no \; failure \end{cases} \tag{2.5}$$

6. Interlaminar compression failure for $\sigma_{33} < 0$

$$\left(\frac{\sigma_{33}}{Z_C^2}\right)^2 = \begin{cases} \geq 1 \; failure \\ < 1 \; no \; failure \end{cases} \tag{2.6}$$

Where, σ_{ij} denote the stress components and the tensile and compressive allowable strengths for lamina are denoted by subscripts T and C, respectively. X_T, Y_T, Z_T denotes the allowable tensile strengths in three respective material directions. Similarly, X_C, Y_C, Z_C denotes the allowable tensile strengths in three respective material directions. Further, S_{12}, S_{13} and S_{23} denote allowable shear strengths in the respective principal material directions.

2.3 Finite element analysis

2.3.1 Introduction

Finite element analysis (FEA) has become very common in all kind of business and is now the basis of a multibillion dollar per year industry. Numerical solutions to even very complicated stress problems can now be obtained routinely using FEA.
In spite of the great power of FEA, the disadvantages of computer solutions must be kept in mind when numerical methods [8]. They do not necessarily reveal how the stresses are influenced by important problem variables such as materials properties and geometrical features. Furthermore, small errors in input data can produce wildly incorrect results that may be overlooked by the analyst. Perhaps the most important function of theoretical modeling is that of sharpening the designer's intuition; users of finite element codes should compare the computer simulation with experimental analysis as often as possible.

2.3.2 Finite Element Analysis concept

Finite element analysis is based on the Finite Element Method (FEM). The finite element method (FEM) is a numerical tool for finding approximate solutions to differential

equations [7]. In the same way a circle can be obtained connecting tiny straight lines, FEM has the methods for connecting many equations calculated in small subdomains (elements) into a more complex equation valid for larger domains.
Even though it is difficult to quote a date for the invention of the finite element method, it is known that it originated from the need to solve complex elasticity and structural analysis problems in civil and aeronautical engineering. It was in the late 50s and early 60s when this method began to take off. It is remarkable that NASTRAN, a software still used today by many engineering companies was released in 1968 by NASA.
The approaches used by the pioneers of this field were different but they shared a essential characteristic, mesh discretization. The division of a continuous domain into a set of sub-domains, known as elements.

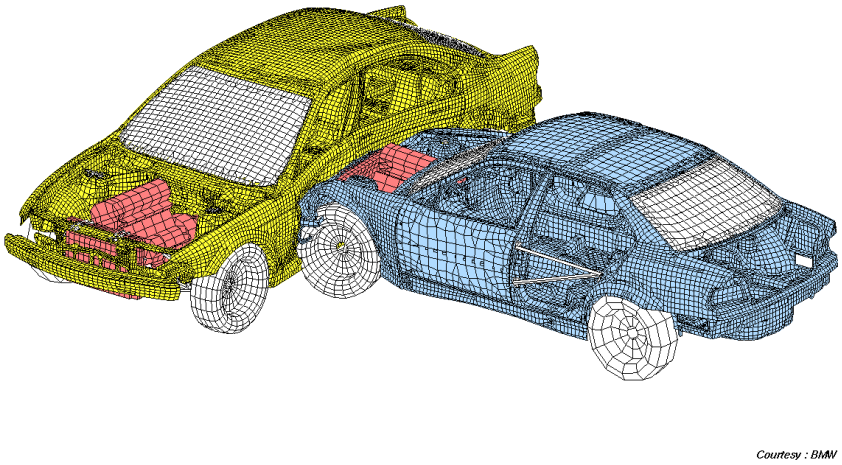

Figure 2.7: Complex part divided in tiny elements

Any model, no matter how complex it may be can be split into simpler and smaller parts, elements.

The subdivision of a whole domain into simpler parts has several advantages:

-Accurate representation of complex geometry
-Inclusion of dissimilar material properties
-Easy representation of the total solution
-Capture of local effects.

A typical finite element method code includes:

1) Domain division.
2) Set recombination.

1- Domain Division: Element equations are simple equations that approximate in the subdomain the original (and complex) equations to be studied. Original equations are usually partial differential equations (PDE) which are approximated locally with:
-A set of algebraic equations for steady state problems.
-A set of ordinary differential equations for transient problems.
These set of equations are the element equations. They are linear if the PDE where the come from is linear, and viceversa. Steady state problems are solved using numerical linear algebraic methods, while differential equation sets are solved by numerical integration using standard techniques such as Euler's method or the Runge-Kutta method.

2- Set recombination: A global system of equations is generated from the element equations through a transformation of coordinates from the subdomains' local nodes to the domain's global nodes. This transformation includes appropriate orientation adjustments as applied in relation to the reference coordinate system. The process is often carried out by FEM software using coordinate data generated from the subdomains.

Finite Element Analysis (FEA) [6]

The computational tool used to perform engineering analysis is called Finite element analysis (FEA). In practice, a finite element analysis software usually consists of three principal steps:
1. Preprocessing: The user constructs a model of the part to be analyzed in which the geometry is divided into a number of discrete sub-regions, or elements, connected at discrete points called nodes. Certain of these nodes will have fixed displacements, and others will have prescribed loads. These models can be extremely time consuming to prepare, and commercial codes vie with one another to have the most user-friendly graphical 'preprocessor' to assist in this rather tedious chore. Some of these preprocessor can overlay a mesh on a preexisting CAD file, so that finite element analysis can be done conveniently as part of the computerized drafting-and-design process.
2. Analysis: The data-set prepared by the preprocessor is used as input to the finite

element code itself, which constructs and solves a system of linear or nonlinear algebraic equations. Commercial codes usually have very large element libraries, with elements appropriate to a wide range of problem types. One of FEA's principal advantages is that many problem types can be addressed with the same code, merely by specifying the appropriate element types from the library.
3. Post-processing: In the earlier days of finite element analysis, the user would pore through reams of numbers generated by the code, listing displacements and stresses at discrete positions within the model. It is easy to miss important trends and hot spots this way,and modern codes use graphical displays to assist in visualizing the results. A typical post-processor display overlays colored contours representing stress levels on the model,showing a full-field picture similar to that of photo-elastic or moire experimental results.
The method has been generalized since its development for the numerical modeling of physical systems in a wide variety of engineering disciplines, e.g., electromagnetism, heat transfer and fluid dynamics or bioengineering.

2.3.3 Element definition

When working with finite element models there is quite a important thing to take into account [9], whether to model the part as a shell or as a solid. Each of them have a different formulation and its advantages and disadvantages.

Shell elements:

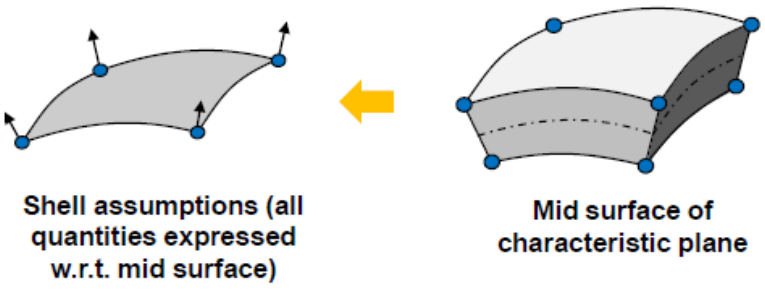

Figure 2.8: Solid to shell simplification

-Shell elements are to be used when one dimension is much smaller than the other two

(about 20 times say some experts).
-They are easier to create, only defining the mid-line (or plane) and then adding a thickness to it.
-Shells cannot carry out of plane loads.
-Shells are not good when bending is considered unless different integration points are considered across the thickness (in this case they are basically treated as a solid but out of plane loads are still disregarded)
-Processing and computation is faster due to the reduced geometry.

Solid elements:

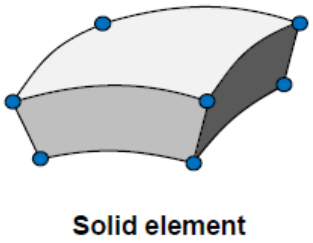

Figure 2.9: Solid formulation scheme

-They are closer to the reality and easier to understand.
-With solids boundary conditions are more realistic (which avoids computational noise) since boundary conditions for solids (faces) are better defined as with shells (edges).
-Solid elements are actually better in all aspects but in computational weight.

2.3.4 Solving method. Implicit vs explicit:

A static analysis, like a stress analysis in FEA, is done using the simple linear equation [A]$\vec{x}$=B. In such analysis time does not play any role [9]. On the other hand a dynamic analysis (or transient or modal analysis also) follows a more complex governing equation which is like:

$$[M]\vec{x''} + [C]\vec{x'} + [K]\vec{x} = \vec{F} \tag{2.7}$$

Implicit solution is one in which the calculation of current quantities in one time step are based on the quantities calculated in the previous time step. This is called Euler

Time Integration Scheme. In this scheme even if large time steps are taken, the solution remains stable. There is a disadvantage, and it is that this algorithm requires the calculation of inverse of stiffness matrix, since in this method we are directly solving for $\vec{x}$. And calculation of an inverse is a computationally intensive step. This is especially so when non linearities are present, as the Stiffness matrix it self will become a function of x.

In an explicit analysis, instead of solving for $\vec{x}$, we go for solving $\vec{x''}$. Thus we bypass the inversion of the complex stiffness matrix, and we just have to invert the mass matrix [M]. In case lower order elements are used, which an explicit analysis always prefers, the mass matrix is also a lumped matrix, or a diagonal matrix, whose inversion is a single step process of just making the diagonal elements reciprocal. Hence this is very easily done. But disadvantage is that the Euler Time integration scheme is not used in this, and hence it is not unconditionally stable. So we need to use very small time steps.

Due to the non-linear behavior of the simulations performed in this project (it uses contacts and non-linear material model that includes plasticity and rupture), explicit formulation was used taking care of the following characteristics:

-Maximum stable time step in an explicit simulation is given by the Courant number, which depends on the length of the smallest element and, also, on the material properties. One excessively small element will reduce the stable time step for the whole model:

$$\Delta t_{max} = \frac{L}{c} = \frac{L}{\sqrt{\frac{E}{\rho}}} \tag{2.8}$$

Where L is the length of the smallest element, c is the sound speed in the material, E is the Young modulus and ρ is the density of the material.

-Time steps used in the simulations have been checked to accomplish this Courant criterion.
-Energy conservation of each simulation run has been checked to assure its stability.

CHAPTER 3

3. Axial Beam Crushing

3.1 Test Description

The specimen to be tested is an axial Aluminum beam with square cross section (60mm x 60mm) which is 2mm thick and 250mm long. The aluminum used was Al 6063T5, a typical Aluminum used in automotive industry. Aluminum 6063 is an aluminum alloy mixed with magnesium and silicon. It has good mechanical properties and it easily welded.

The Aluminum beam is impacted with a carrier with is hydraulically forced. The carrier moves through rails so that only axial movement is considered (when it crashes it could move otherwise). The beam is clamped to a big-metal non moving part. The composite is bonded to the aluminum for the hybrid crushing with an epoxy adhesive.

The specimen was tested according to the RCAR regulation for low speed crashing tests, the bumper and the crash box have to absorb the energy corresponding to a mass of 300Kg moving at 16Km/h, which is around 2960J.

As there are always two beams per bumper, the necessary energy to be absorbed by one is 1480J. In the experiment this energy was modeled by a moving mass of 250Kg at 3.55 m/s which actually adds up to 1575J, 6.42% more than the regulation limits. In the test the bar was impacted by a rigid carrier arranged in a disposition as shown below in

figure 3.1

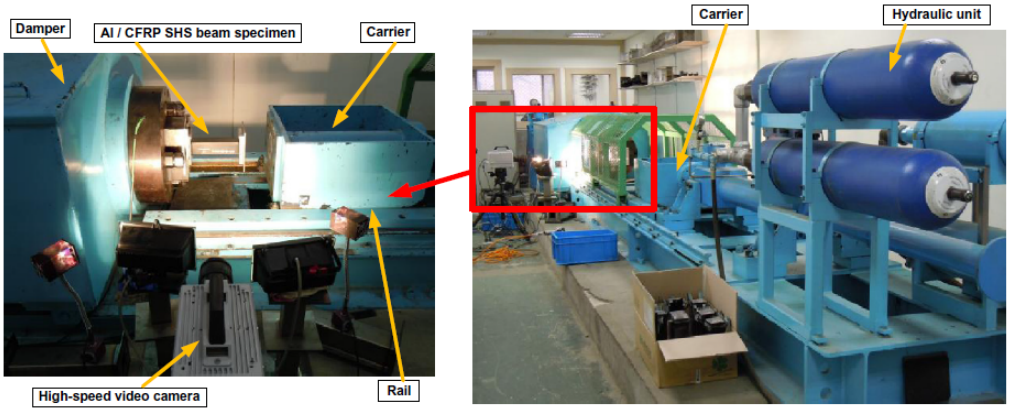

Figure 3.1: Test arrangement

For the aluminum beam, its collapsing sequence can be observed in figure 3.2 where lobes formation are strictly related with the force peaks seen in figure 3.3.

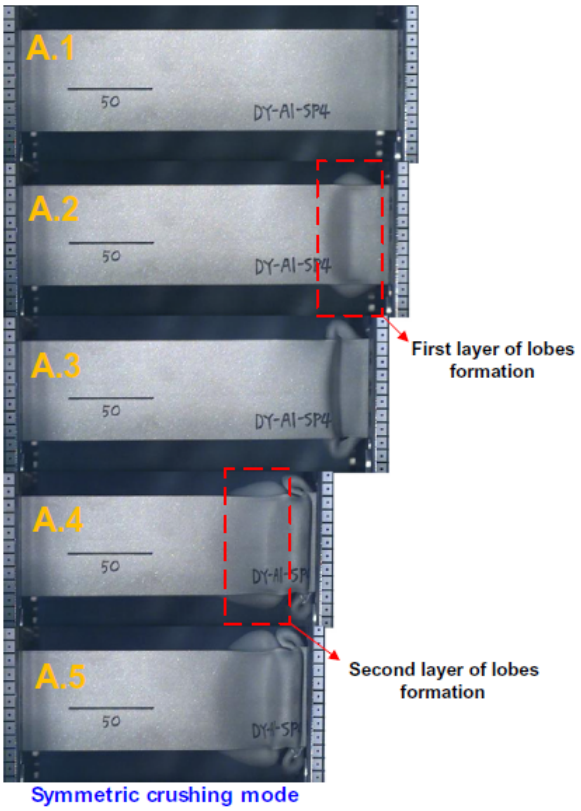

Figure 3.2: Aluminum collapse sequence

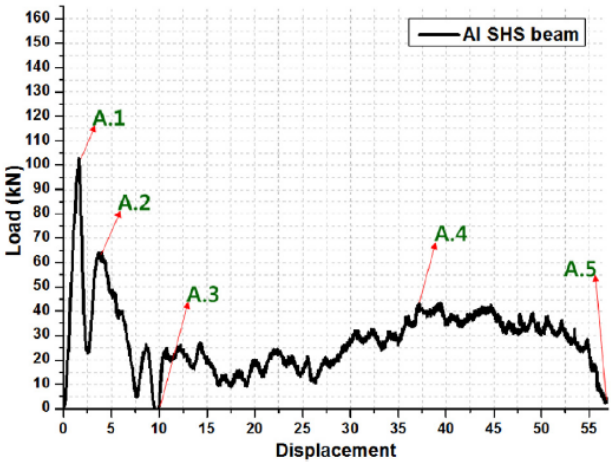

Figure 3.3: Force vs Displacement for Aluminum

The aluminum bar is then covered with carbon fiber reinforced plastic (CFRP). Different plies sequences are tried in order to look for the best result.
The stacking sequences studied in the test are: $[0°]_2$, $[0°]_4$, [90°]2 , $[90°]_4$,$[0°/90°]_2$, $[0°/90°]_4$, $[+45°/-45°]$, $[+45°/-45°]_2$ being the total thickness of the composite layer always 0.4mm.
The one having the best behavior was found to be the one at $[0°]_4$,as it can be seen in the following figure, being able to reduce the displacement up to 25mm.

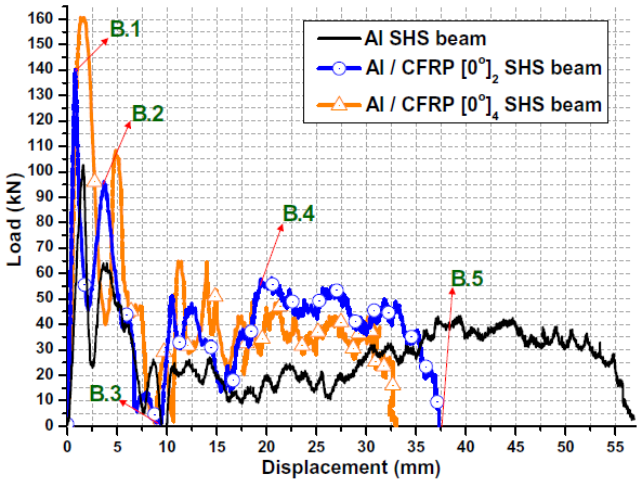

Figure 3.4: Force vs Displacement for Hybrid structure for [0°] degrees ply

In figure 3.5 the crashed hybrid beam can be seen.

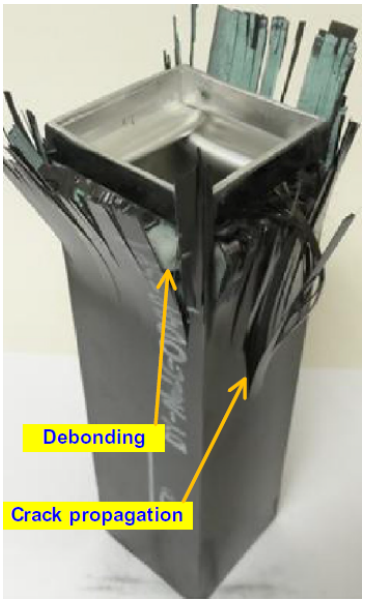

Figure 3.5: Hybrid structure for [0°] degrees plies

3.2 Model Description

The model was reproduced trying to be as close as possible to the experiment. First of all the geometry was designed. For doing so different parts were modeled. Then material properties were added. The next step was to set the boundary conditions and the interaction between parts. Finally the variables of interest were requested.

3.2.1 Geometry

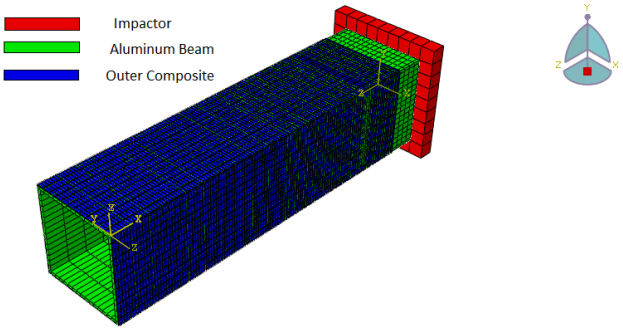

Figure 3.6: Whole model assembly

The composite was modeled as two different parts so that debonding could be studied. The outer composite is the blue one that can be seen in figure 3.6 and the inner one cannot be appreciated since it is 0.2mm thin. The blue part corresponds with the aluminum beam and red part with the steel impactor. A precise geometric description is given below:

-**Aluminum beam** (60mm x 60 mm x 250mm and 2mm thick)
-**Impactor (Carrier)** (80mm x 80mm x 10mm)
-**Outer Composite** (60mm x 60 mm x 230mm and 0.2mm thick)
-**Inner Composite** (60mm x 60 mm x 230mm and 0.2mm thick)

3.2.2 Mesh

Mesh is always a tricky part to work with when doing models with finite element method softwares. This is due to mesh convergence which is not a trivial concept. It may appear clear that the more elements the better since the model will be then closer to reality. However there is a point in which an excessive number of elements may worsen the quality of the results, this is a result of error accumulation.

This can be seen clearer in figure 3.7

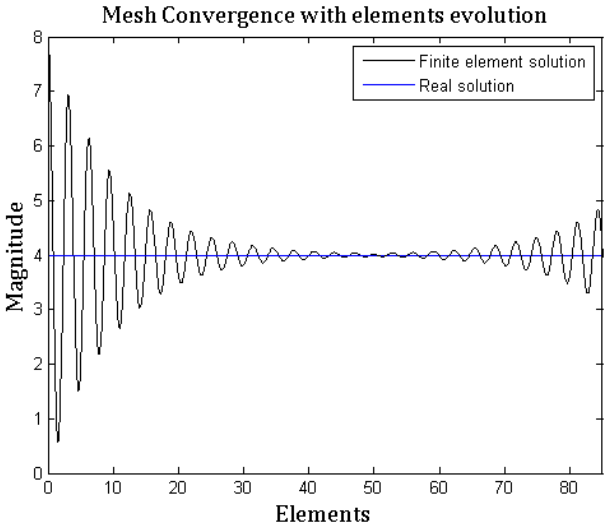

Figure 3.7: Mesh convergence

In principle the accuracy of the results are increased with the number of elements. This is a logical thinking since the more elements are included, the closer the simulation is to

the reality. There is a point in which the increase of elements does not vary the results. However, if mesh is increased too much the solution will start to become worse due to the accumulation of error coming from an excessive number of nodes.
The approach for choosing a good mesh consist on picking an initial mesh which quality will depend on engineer's experience. The following step would be then to try different meshes. One improved and another worsen in order to check where we are in the upper figure. Once we know which tendency we should follow, we know in which direction to move on.
For both softwares, the selected mesh is the same taking into account that the following pictures are for solids in which 2 elements across the thickness are defined and in shell elements only 1 is taken into consideration.

For the aluminum beam the selected mesh is visible in 3.8

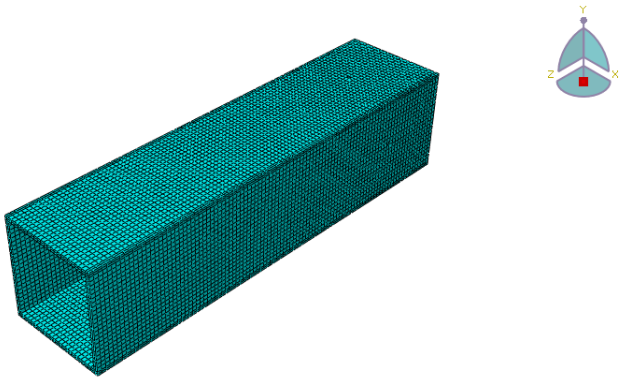

Figure 3.8: Mesh for Aluminum beam

This includes 100 elements across the span, 25 in each side of the square and 2 elements across the thickness amounting to 20000 elements.

As it was commented before, meshing a solid is more complex than doing it for a shell. An example of what it is need to be done is seen in 3.9
Partitions in the solid had to be made so that the mesh could be uniform and straight. Otherwise as the top length is lower than the inner angular elements would be created adding inaccuracy to the model.
Dividing a solid in several sub-parts has disadvantages such as increase of interactions (when clamping or working with the plate against solid interaction) which in the end leads to more computational time and errors.

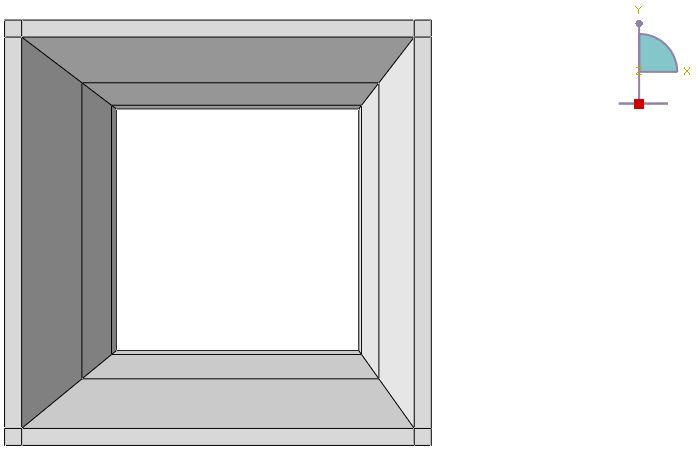

Figure 3.9: Aluminum partition needed for mesh

The impactor plate has the following mesh observed in 3.10

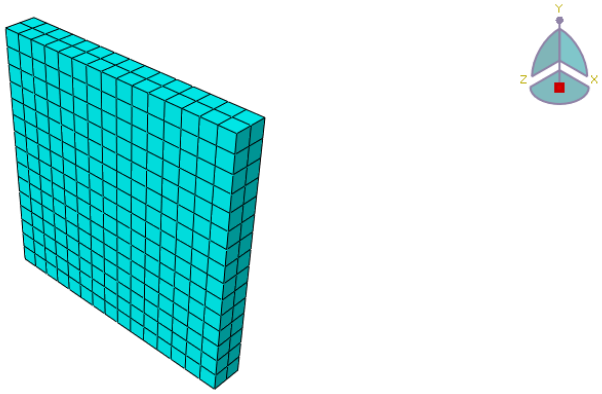

Figure 3.10: Impactor plate mesh

Which consists on 2 elements across the thickness and 15 in each side of the square cross section being 450 the total number of elements.

When the composite was introduced, the Aluminum mesh had to be reduced due to the excessive new of new nodes coming from the composite parts. This mesh has 3500 elements, it is much more reduced than the previous which had 20000. Nevertheless, this mesh was optimized so that in the critical zone for aluminum bucking it was as fine as possible without sacrificing computational time. It can be seen in the following figure 3.11

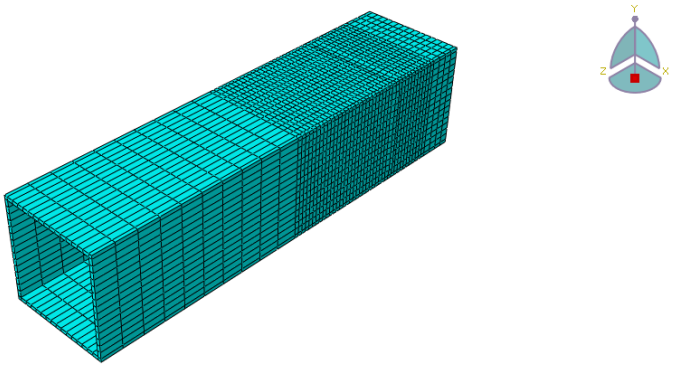

Figure 3.11: Reduced Aluminum Mesh

The outer composite part can be observed in figure 3.12

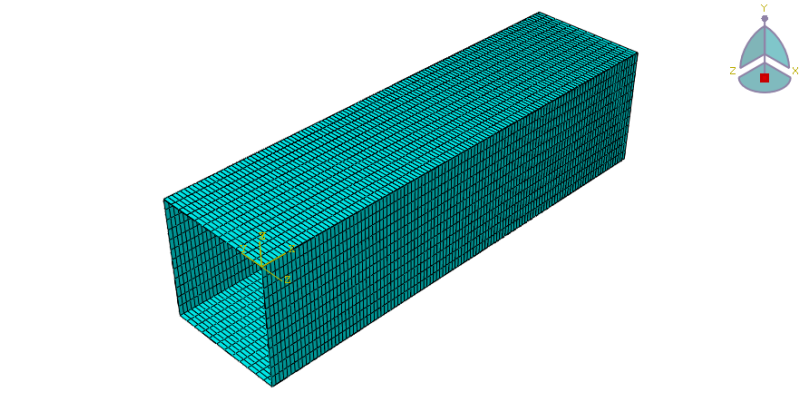

Figure 3.12: Outer composite Mesh

It has 2 elements across the thickness, 12 elements per square side and 116 elements across the span. Amounting to 12992 elements.

The inner composite part has the same number of elements as the outer one. Even though the dimensions are slightly different, as the difference is almost negligible the size of the elements was chosen to be the same.

3.2.3 Material properties:

Part 1, Aluminum beam (60mm x 60 mm x 250mm and 2mm thick)

Material properties: Al 6063T5
Density, ρ=2700 Kg/m3
Young Modulus, E=57.1 GPa
Poisson Ratio, ν=0.33

As the problem is highly plastic, these properties had to be included. This was done parametrizing the following Stress-Strain curve 3.13

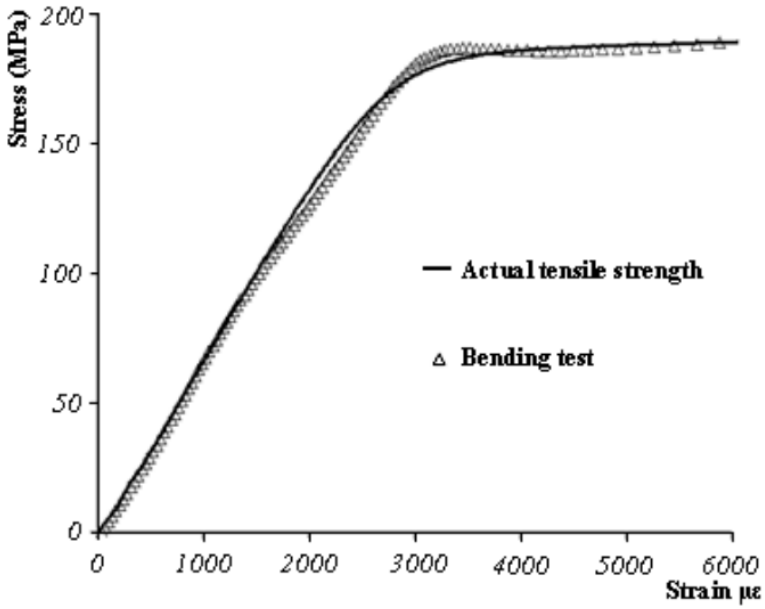

Figure 3.13: Stress-Strain curve for Al 6063T5

Part 2, Impactor (Carrier) (80mm x 80mm x 10mm)

The impactor was modeled in a relatively thin plate with a huge density in order to have the same mass as the one in the test (250 Kg). A much smaller part is easier to model and reduces the integration time since less elements are needed. A general steel was chosen for the values of the Young modulus and the Poison ratio.

Density, ρ= 3906250 Kg/m3
Young modulus, E=1930 GPa
Poisson ratio, ν=0.25

Part 3, Inner Composite (60mm x 60 mm x 230mm and 0.2mm thick)

The span is lower here than in the Aluminum beam because in the way the experiment was developed, the composite beam does not suffer the initial impact from the carrier, the composite is only being stressed by the Aluminum beam when is lobes are formed. If the composite sustained the beginning axial impact, it would break in seconds not being able to add any extra load carrying capability.

Density, ρ= 1600 Kg/m3
Poisson ratio, ν=0.33
Elastic properties (different for each direction)

E_{12}= 142.9 GPa
$E_{13} = E_{23}$ = 78 GPa
$G_{12} = G_{13}$ = 38.9 GPa
G_{23} = 31.12 GPa

Damage properties (for Hashin failure criteria)

X_T = 2036.8 MPa
X_C = 1027MPa
Y_T = 62.5 MPa
Y_C = 285 MPa
$S_{12} = S_{13} = S_{23}$ =120 MPa
Z= 50 MPa

Part 4, Outer Composite (60mm x 60 mm x 230mm and 0.2mm thick)

Different composite parts were created to allow for debonding. Material properties are the same as for the previous composite.

3.2.4 Boundary and initial conditions scheme

In the following picture 3.16, the initial conditions and boundary conditions can be seen:

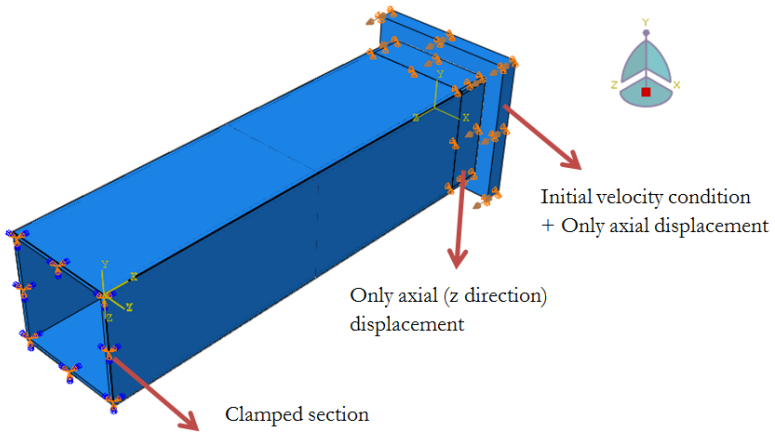

Figure 3.14: b.c and i.c display

Contact:

Solid interactions:
Hard contacts were defined amongst the parts so that the could interact/impact with each other and amongst themselves.

-Adhesive behavior
To reproduce this in Abaqus or in Pam-Crash, cohesive interactions were defined which allow for debonding once the glue is broken.
The Aluminum and the Composite are joined with FM 300 Epoxy film adhesive [10]. An adhesive which is recommended by the developer for:

- Metal-to-metal bonding
- Composite-to-composite bonding
- Composite-to-metal bonding
- Composite surfacing

The adhesive has the following properties:

Normal Stress (S_{12}) 55 MPa
Shear Stress (S_{13},S_{23}) 68 MPa
Normal fracture energy 300J
First and second shear fracture energy 2023J

Debonding is modeled in the softwares with the Paris' law. Paris' law is one of the most popular crack growth models used for fracture mechanics. It relates the stress intensity factor to the crack growth under a fatigue or stress regime.

$$\frac{da}{dN} = A(\Delta\sigma\beta\sqrt{\pi a})^n \tag{3.1}$$

Where a is the crack growth [m], N the number of cycles, A [m/cycle] and n [-] are material constants, $\Delta\sigma[Pa]$ the variation of stress and β [-] is a constant depending on the crack mode.

The stress intensity factor, ΔK is defined as $\Delta K = \Delta\sigma\beta\sqrt{\pi a}$ The crack growth is divided in 3 regions. In the first it growths very slowly and the equation overestimate the actual result. In the second one it growths linearly and it approaches really good the real behavior. In the last one in which it growths really fast and the model is not able to predict it properly. The Paris's law can be understood better taking a look at figure 3.15.

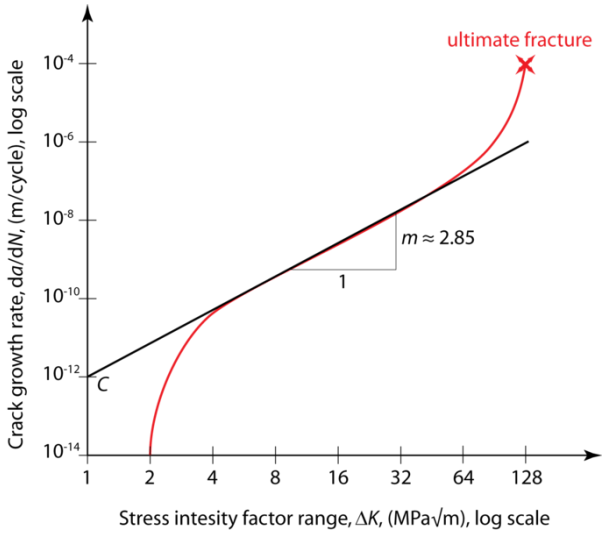

Figure 3.15: Paris Law

Boundary Conditions:

Clamped beam: For simulating the clamped part of the beam, all degrees of freedom (rotational and displacement) were limited for the latter elements of the Aluminum and Composite bars.

Axial behavior: No lateral displacement was allowed for the impactor plate simply by constraining the movement in the x and y plane. This is done in the experiment by forcing the carrier to move through rails.

Aluminum bar fixing: No displacement out of plane for the first 20mm of the Aluminum beam. This was done constraining once again x-y directions to reproduce the way the part is held in the experiment which can be seen in the following pictures:

As the bar is inside the holder the first 20mm of the section do not get deformed:

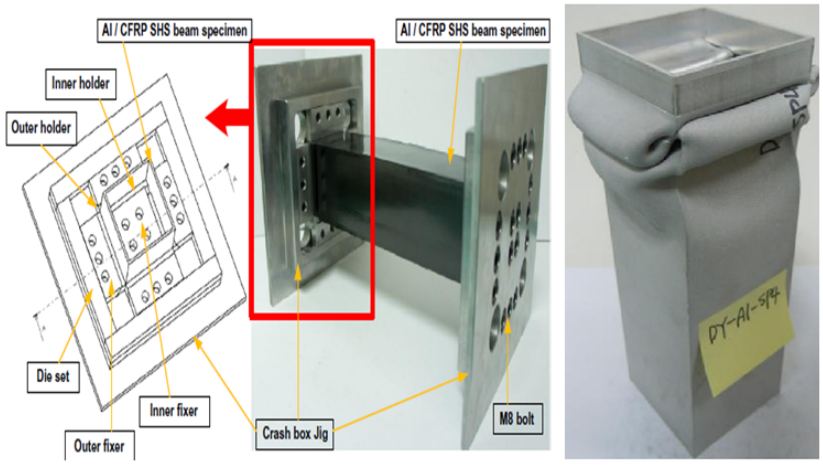

Figure 3.16: a) Beam arrangement. b) Aluminum beam after impact

Initial Conditions:

The initial velocity was simulated by assigning the plate an initial condition of 3.55 m/s.

Output requests and variables to control:

The metrics that need to be obtained to compare with the test results are the force in the contact section between the plate and the beam, the deformation of the beam and the energy absorbed.

-The force is obtained by demanding it (this is done differently for each software) in the contact section.

-The deformation of the beam is obtained by monitoring the evolution of the position of a node of the Aluminum beam which belongs to the first 20mm where the x-y directions are restricted.

-The energy absorbed by the beam is simply the integral of the force vs displacement curve.

The need for mesh distortion:

There is an important concept to be introduced when working with finite element methods, sometimes there is a problem coming from the perfection on the mesh definition. For example for a software that has been tested for many years such as NASTRAN, a beam loaded uniaxially does not buckle but is compressed widen due to Poisson effects. In the reality it is known that this experiment will result with a hundred percent certainty in a buckling problem.

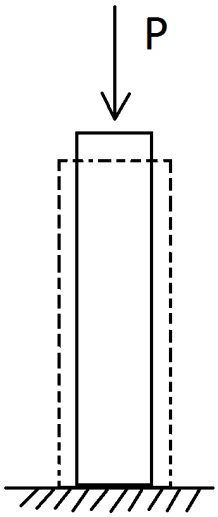

Figure 3.17: Undistorted beam - No buckling

I was finding the same problem in my model. If the mesh was undistorted, a spurious mode would appear:

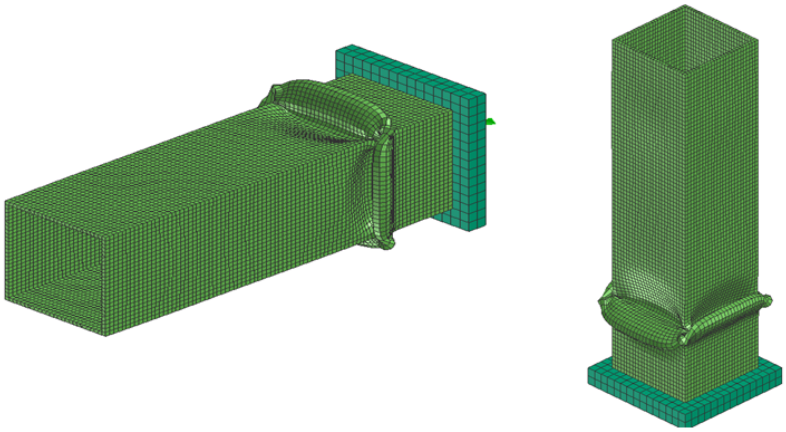

Figure 3.18: Spurious mode. Views 1 and 2

This unreal deformation mode is obtained for both softwares (Abaqus and Pam-Crash) and it is coming from the lack of any preference for lobes formation. In the moment the beam has any preferred orientation, then the real crashing shape appears.
For the Aluminum beam problem, with the displacement of a node in each face of the cross section 0.5mm the aimed shape would already appear. However, in the model with composites, this mesh distortion was not enough and the same spurious as before would appear. This is coming from the extra stiffness added from the composite layer. For this case displacing several nodes in each face was needed (again 0.5 mm). The distorted mesh for the composite layers can be seen in figure 3.19

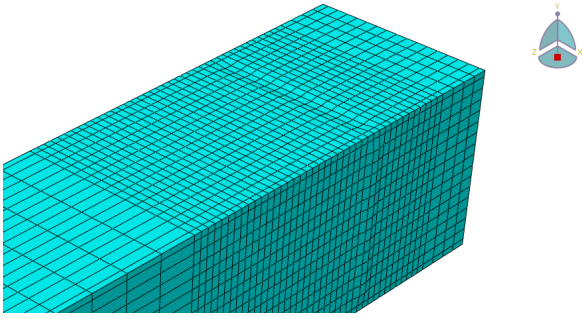

Figure 3.19: Distortion needed for lobes formation

Composite failure in Abaqus:

Abaqus failure treatment was not good enough for the purpose of this project (results were inaccurate) so a FORTRAN subroutine was included. This subroutine applies the Hashin failure criteria that was explained in 2. The subroutine works as intermediary between Abaqus and an Intel compiler. At every step Abaqus passes the values of the stresses to the subroutine. The subroutine transforms it to local axes, through matrices transformations, then applies the Hashin failure criteria and finally returns the values of the stresses and deformations to the previous axes before returning them to Abaqus. The subroutine was built by the UC3M department “Mecánica de medios continuos y teoría de estructuras”. [14] [12]

CHAPTER 4

ALUMINUM CRUSHING BEAM STUDY. MODEL RESULTS

4.1 First Approximation

With energy conservation, a first order approximation of the energy absorption behavior can be computed. This is a linear theory and only predicts the elastic behavior. The impacting energy is 1480J $\frac{mv^2}{2}$. Assuming energy conservation (which means no heating, no friction and no damping) the impacting energy is equal to $\frac{kx^2}{2}$. k, the stiffness for a continuous system can be modeled as k=AE/L where A is the cross sectional area of the aluminum, E is the Young modulus and L is the length. $A = (60^2 - 58^2)mm^2$ and the Young modulus is 57.1 GPa. As all the variables are known, it is possible to compute the predicted displacement. $x = \sqrt{\frac{mv^2}{k}} = 4mm$.

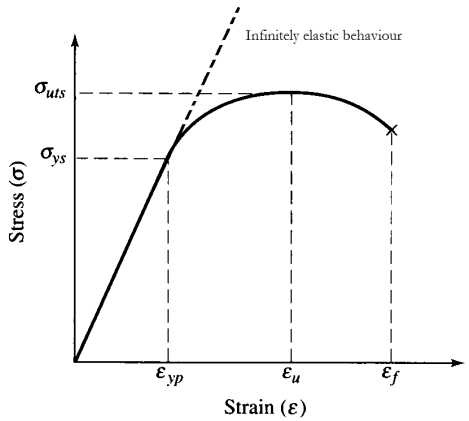

Figure 4.1: Undistorted beam - No buckling

4.2 Softwares Analysis

In the following sections the results results obtained for Pam-Crash and Abaqus will be exposed. For every software computations were performed for solid and shell elements.

4.3 Solid Aluminum Abaqus

In the following picture a comparison between the crushing sequence can be observed for Abaqus and the test.

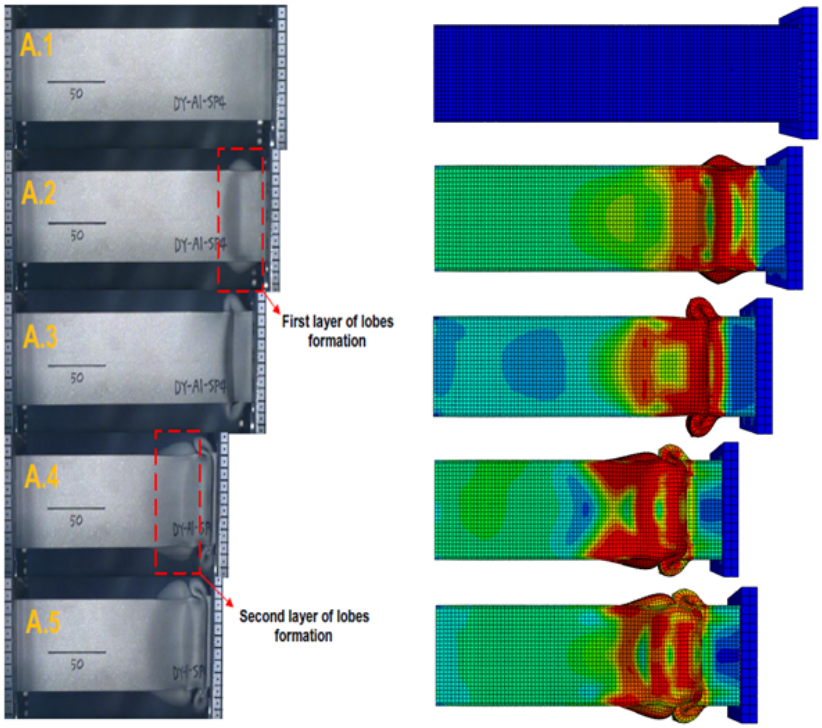

Figure 4.2: Aluminum Collapse Sequence. Test vs Simulation

The color scale in Abaqus represents the Von Mises criteria which is a measure of the stress. The heater colors correspond with zones that have plastified and are undergoing non-linear deformation and the coldest regions are those undergoing barely no stresses.

However visual comparison does not say much apart from saying that the failure mode is the correct one. In order to compare, histograms are needed.
Integrating the curve, the impulse is obtained. An useful magnitude to compare between the different models is the impulse. The comparison will be performed once all the models

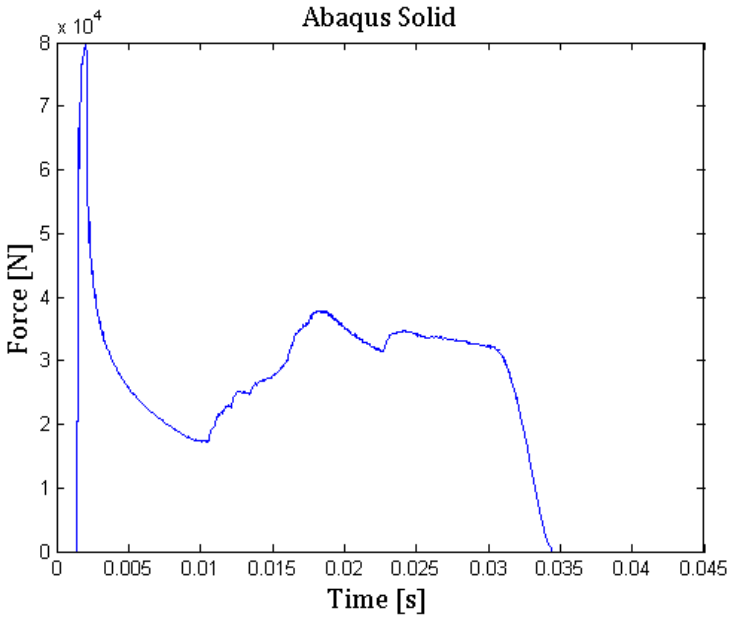

Figure 4.3: Force vs Time. Abaqus Solid

have been presented.

Impulse: 960Ns

4.4 Shell Aluminum Abaqus

Visually we can check that the failure mode is adequate.

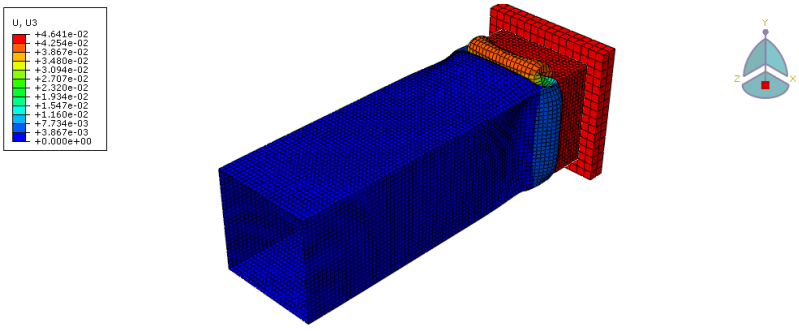

Figure 4.4: Deformed aluminum. Abaqus Shell

The curve of force vs time is apparently similar to the upper.
However the impulse is much smaller than the previous and this is coming from the variation in the peak value. An interesting thing to remark here is, as it was explained

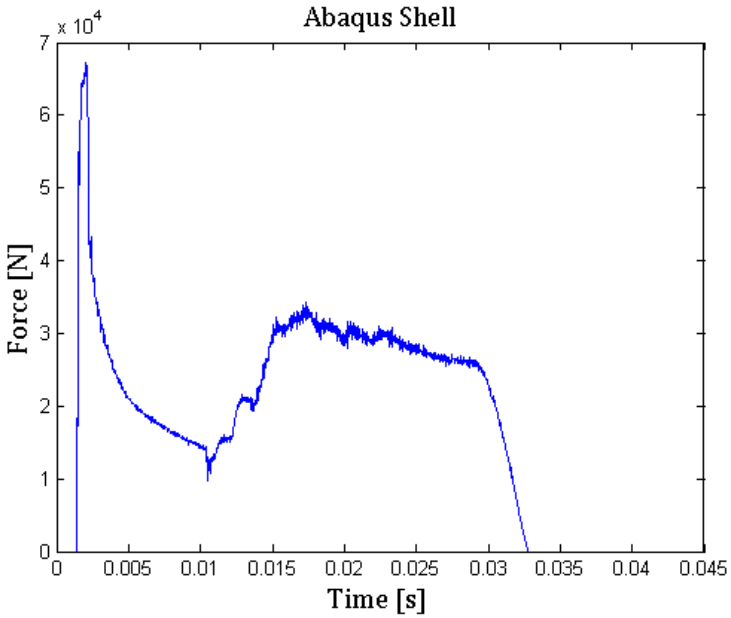

Figure 4.5: Force vs Time. Abaqus Shell

above, that the signal has more noise than the previous. This is coming from the interaction between the shell beam and the solid impactor.

Impulse: 774 Ns

4.5 Solid Aluminum Pam-Crash

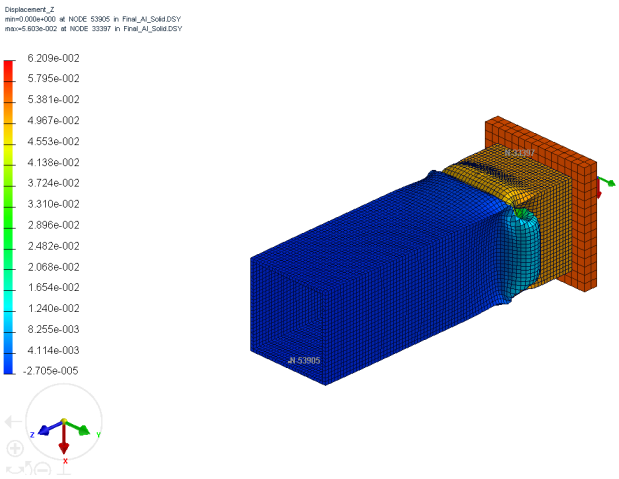

Figure 4.6: Deformed beam. Pam-Crash solid

The force vs time figure looks similar to the previous ones.

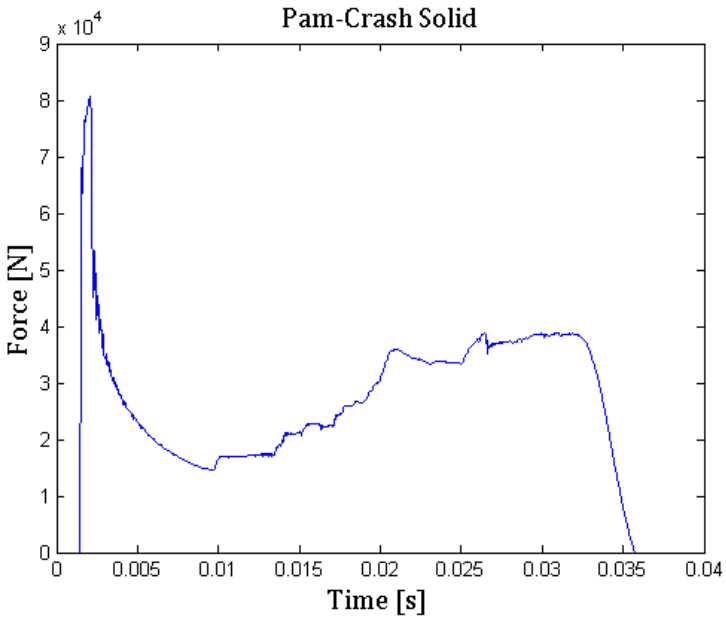

Figure 4.7: Force vs Time. Pam-Crash Solid

This signal is for this case cleaner than for the previous. And the value of the impulse is very close to the solid Abaqus value and so is the value of the peak.

Impulse: 966 Ns

4.6 Shell Aluminum Pam-Crash

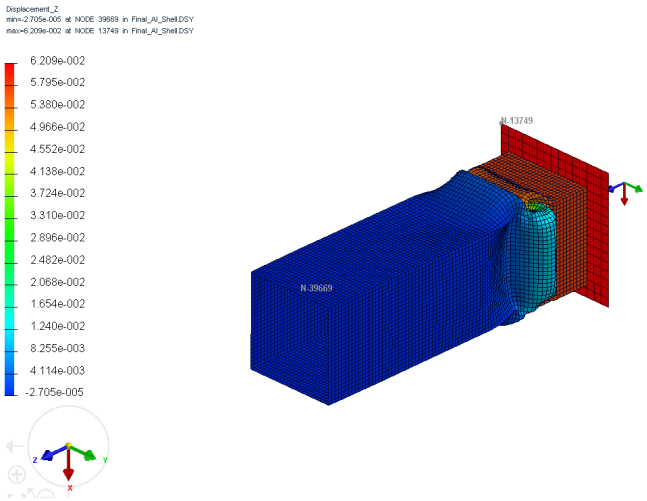

Figure 4.8: Deformed beam. Pam-Crash Shell

The value of the peak force is similar to that of Abaqus solid and Pam-Crash solid.

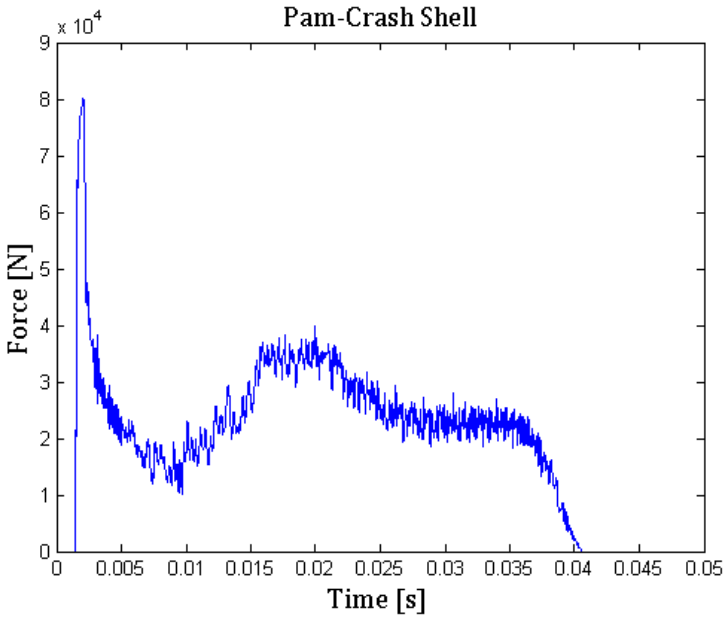

Figure 4.9: Force vs Time. Pam-Crash Shell

The signal is much noisier since in this case the impactor was modeled as a shell to prove precisely that the signal noise comes from the shell interactions. The value of the impulse is very close to those of Abaqus Solid and Pam-Crash solid. Impulse: 959 Ns

4.7 Results Comparison

From the upper graphs, a feeling that there is something wrong in the Abaqus shell model is got since its value of the impulse is quite different from the others. To ensure that, lets take a look at all the results together. Now the force is plot against the displacement and the data of the test is added.

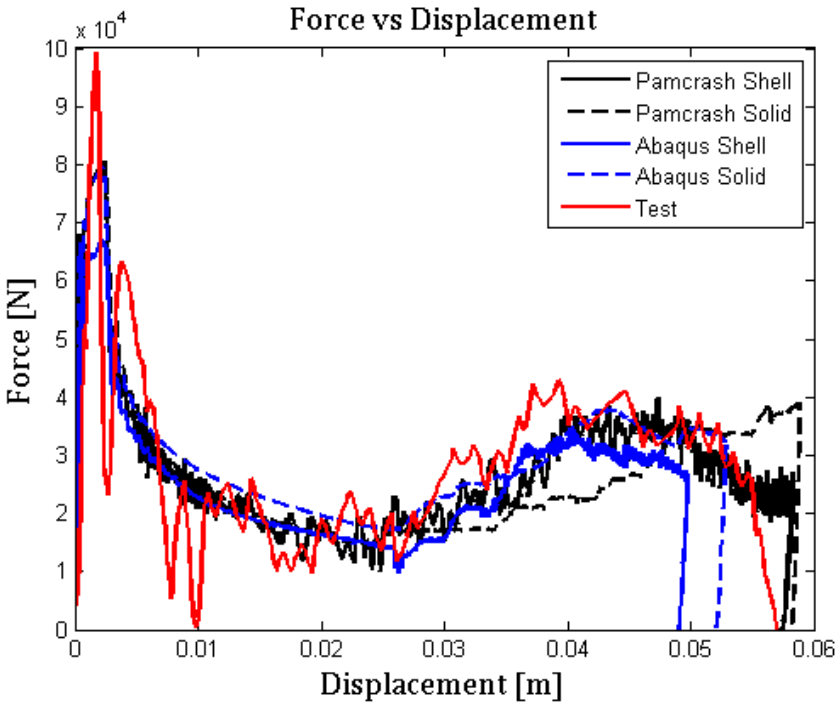

Figure 4.10: Force vs displacement comparison. Test vs Simulations

Integrating the upper curves to obtain the absorbed energy of impact:

Table 4.1: Comparison of the Energy Absorbed for the Aluminum bar

Case	Shell	Solid
Abaqus	1.25 KJ	1.56KJ
Pam-Crash	1.57 KJ	1.56 KJ
Test	1.59 KJ	

From these results it can be ensured that the Abaqus shell model is not working properly since its results are quite far from the other simulations and from the test. On the

other hand the remaining results are excellent since they are all very close amongst simulations but also really close to the value obtained in the test.
It can be seen a different tendency between the simulated graphs and the test one. All the simulated ones rebound. Once the impact is sustained, some of the energy has not been converted into plastic deformation but elastic, forcing the plate to move back and allowing the beam to decompress. In the test this is not happening which means that this energy has gone somewhere else, this could have gone to heating up the beam, friction in the wheels of the carrier or simply energy released trying to move back the carrier and not being able.
From here it can be said that the shell Abaqus model is wrong. The reason why it is not working is due to the lack of thick shell elements in the Abaqus version used. With only two integration points across the thickness, one in the upper face of the shell and another in the lower, it is impossible to compute bending of the element. With this lack of precision, it is impossible to simulate the behavior of the beam.

Comparison amongst softwares:

Table 4.2: Pam-Crash vs Abaqus. Computational data comparison.

	Pam-Crash	Pam-Crash	Abaqus	Abaqus	
	Shell	Solid	Shell	Solid	Test
Total time	1h 29min 15s	1h 21min 20s	3h 20min 29s	2h 6min 36s	
Initial time step (s)	$0.46.10^{-6}$	$0.16.10^{-6}$	$0.43.10^{-6}$	$0.13.10^{-6}$	
Minimum time step (s)	$0.2.10^{-6}$	$0.14.10^{-6}$	$0.0041.10^{-6}$	$0.009.10^{-6}$	
Output files (MB)	79	55	467	227	
Input file (MB)	1.3	2.7	0.9	2.9	
δ_{max} (mm)	58.3	58.9	49.8	52.8	57

The most remarkable thing about this table is the behavior of shell elements. Shells are supposed to be best in terms of computational times and efficiency. However, they are proved to be worse in computational times and files sizes for two completely independent softwares. Comparing softwares results, Pam-Crash's outputs are better than Abaqus'.

Both shell and solid modeled with Pam-Crash predict almost the same displacement as the one from the test (between 1 and 2mm difference). Abaqus solid is a slightly further from the 57mm from the test but it is a very good approximation anyhow.

Models are then validated and found suitable for predicting the global behavior of the structure. Therefore they can be used for optimizing and improving the design before doing real tests which saves efforts and money.

4.7.1 Abaqus vs Pam-Crash

It is interesting to do a comparison between softwares apart from looking at the results obtained with each one. I find that Pam-Crash is a much powerful software but this comes with the problem that there are thousand of parameters controllable in it which makes it really difficult building even a simple model and get it to work. On the other hand, Abaqus is more user-friendly, moving through the different design phases is much simpler and the CAE builder is considerably better which saves a lot of time. Abaqus does not need to fill as many options as Pam-Crash does. Thus, Abaqus will solve a problem using the most complex approach which comes with extra computational time when compared to Pam-Crash as it can be observed in table 4.2.

CHAPTER 5

HYBRID CRUSHING BEAM STUDY

As the Abaqus Shell was disregarded, it was thought that the better option was to continue with the Shell model in Pam-Crash and the solid in Abaqus. With this approximation, the comparison between solid and shell elements was maintained.

Different ply orientations are going to be studied $[0°]_2$, $[0°/90°]_2$, $[90°/0°]_2$ and $[+45°/-45°]_2$. For comparing the results the energy absorption will be addressed.

5.1 Pam-Crash Hybrid model

For Pam-Crash the mesh for the Aluminum beam was not changed since Pam-Crash is less demanding in computational terms than Abaqus.

Pam-Crash does not include the Hashin failure criteria. The subroutine used for Abaqus is done for solid elements so it was not possible to use it here since the composite was modeled as shell elements for Pam-Crash.
Some difficulties were found when modeling the adhesive between aluminum beam and composite laminate. When the cohesive properties were added -with tie command- the model did not work properly and aluminum deformed freely without contacting with the composite and trespassing it. Great time was inverted in trying to fix this but, unfortunately, a solution was not found.

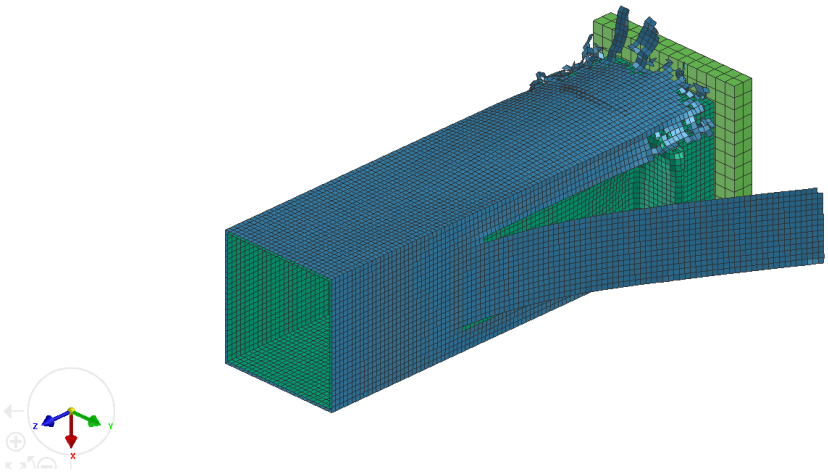

Figure 5.1: Pam-Crash hybrid beam for [0°] degrees plies

Another variation with respect to Abaqus is the use of the Puck method [11] for composite failure due to the lack of Hashin. Even though this is not the reason of the inaccuracy results, this would have lead to a variation of the results with respect to Abaqus if adhesive model have worked properly. Puck in the same way as Hashin, consist on a regime in which the material will not fail.This regime is a function of the stresses and fiber limitations. Puck failure regime is represented as a parabolic shape as it can be seen in 5.2.

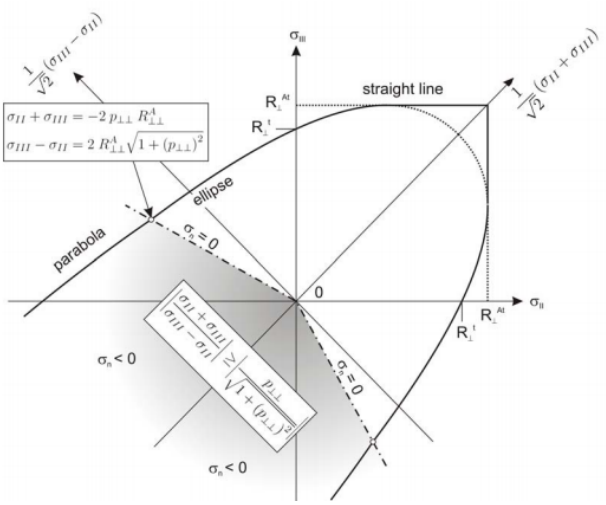

Figure 5.2: Puck equation [11]. Outside of the parabola failure will occur.

5.2 Abaqus Hybrid model

5.2.1 Hybrid model for $[0°]_2$:

For this particular model, two different meshes were tried for the Aluminum beam. The simpler one which is the one used for the rest of the cases (the one which concentrates the elements in the buckling section) and a more complex one which was used for the cases including only the Aluminum beam. The simpler mesh results can be seen in 5.3 and the complex mesh results in 5.4 together with a visual comparison of the tested beam.

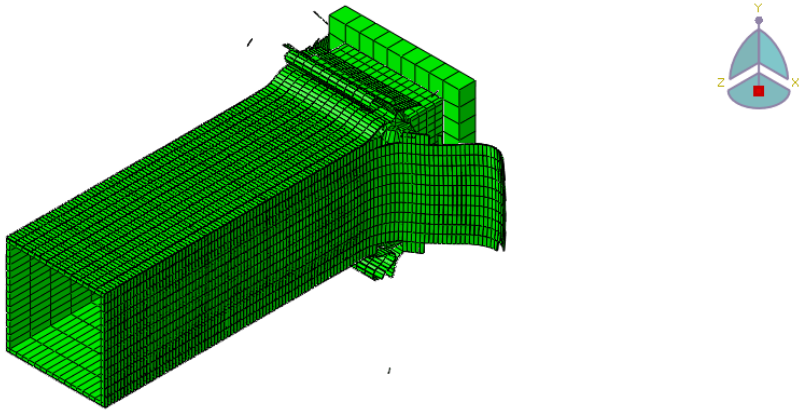

Figure 5.3: Abaqus hybrid beam for [0°] plies. Simpler Mesh

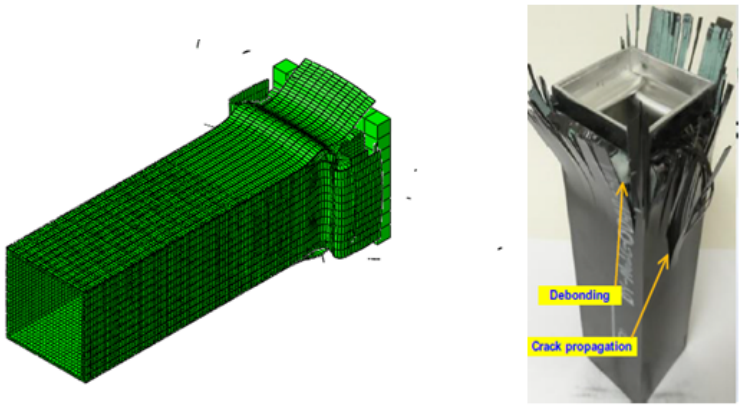

Figure 5.4: Abaqus hybrid beam for [0°] plies. Complex Mesh

For the complex mesh the visual results are much more accurate getting closer to the test results.

However when comparing the results it can be seen that both are close to the test's:

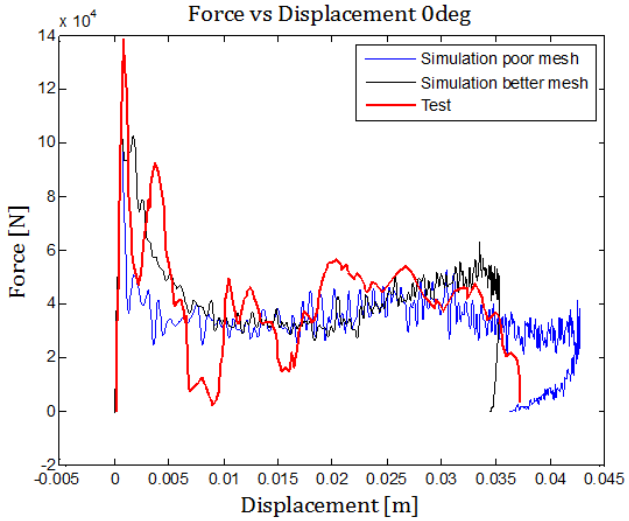

Figure 5.5: Force vs Displacement. Test vs Simulation comparison

As it was addressed before, whenever interaction between elements are included, noise would appear. For this case in which there are more than 12000 composite elements in contact with the aluminum and with another 12000 composite elements, it is understandable the shape of the signal.

To have a clearer visualization of the results, the signals were filtered. The filter is really good for approaching test's result except in the peak which get filtered too much as seen in the following unfiltered signal 5.6. For the following plies orientation, the signal will be also filtered.

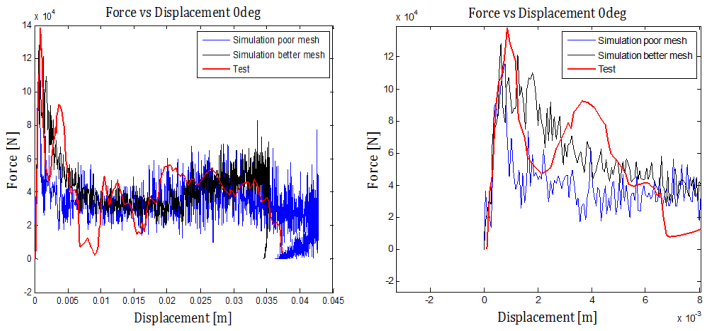

Figure 5.6: Force vs Displacement. Test vs Simulation comparison

5.2.2 Hybrid model for $[90°]_2$:

The visual results do not vary significantly from the ones for 0°

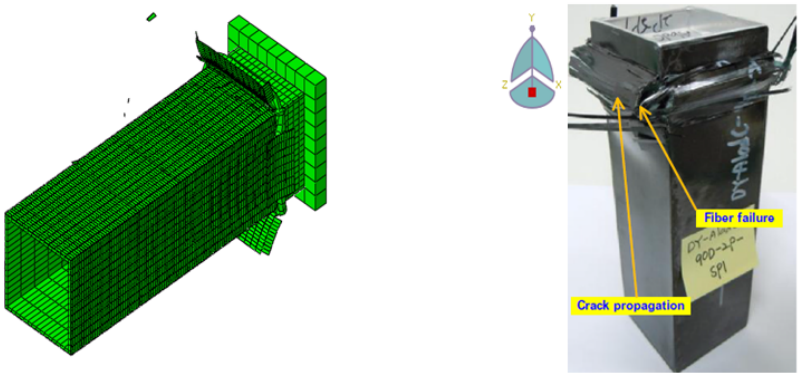

Figure 5.7: Abaqus hybrid beam for [90°] plies. Coarse Mesh

For the force vs displacement curve:

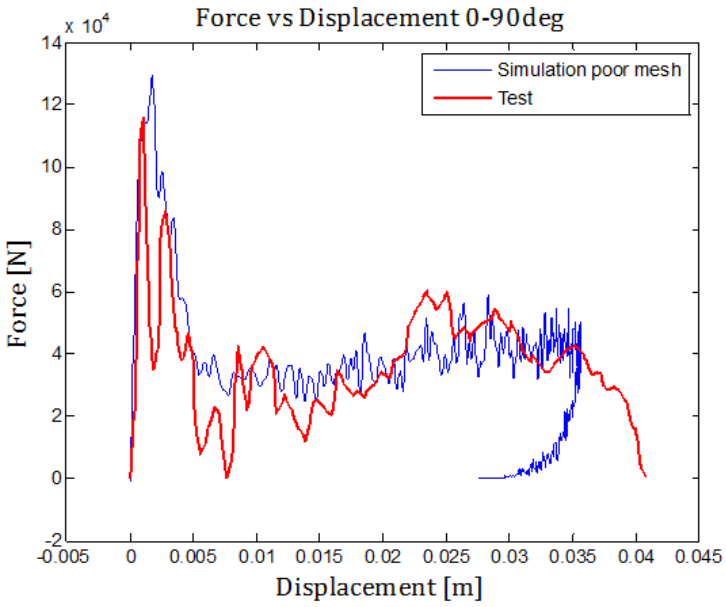

Figure 5.8: Force vs Displacement. Test vs Simulation comparison

Results are very good for this case (even in the filtered peak) up to the rebound in which the simulation predicts too much coming back.

5.2.3 Hybrid model for $[+45°/-45°]_2$:

This is a very particular stacking sequence because in the test it triggers a different failure mode. This is produced by the scissoring effects induced by the 45° fibers.

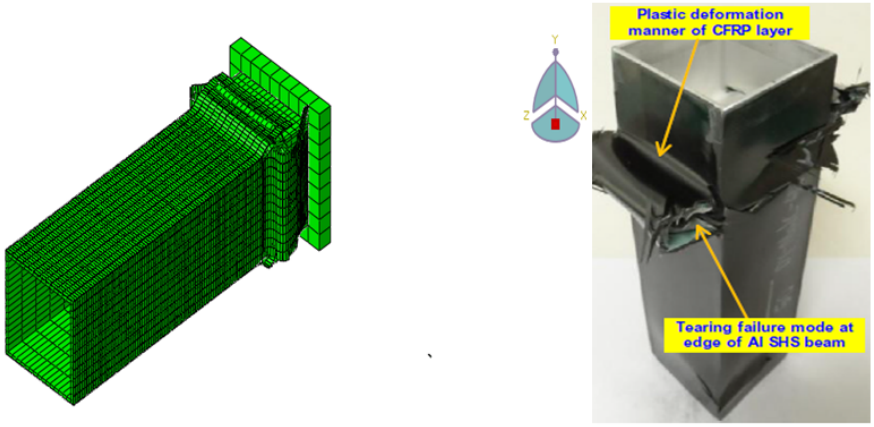

Figure 5.9: Abaqus hybrid beam for $[+45°/-45°]$ plies. Coarse Mesh

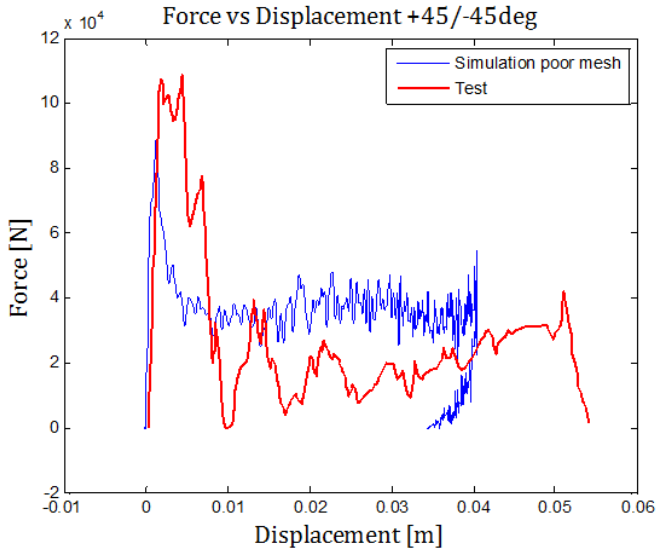

Figure 5.10: Force vs Displacement. Test vs Simulation comparison

A different failure mode occurs in the test for this ply orientation as it can be seen in 5.9. As the model is predisposed (with the mesh distortion) to fail as the previous models do it cannot predict the new mode. If the mesh was undistorted, the spurious mode commented in 3.18 would again appear. As it was impossible to reproduce this particular failure mode, the difference seen between results in 5.10 are understandable.

5.2.4 Hybrid model for $[90°/0°]_2$:

The deformed beam seen in 5.11 has the same aspect as for the previous plies.

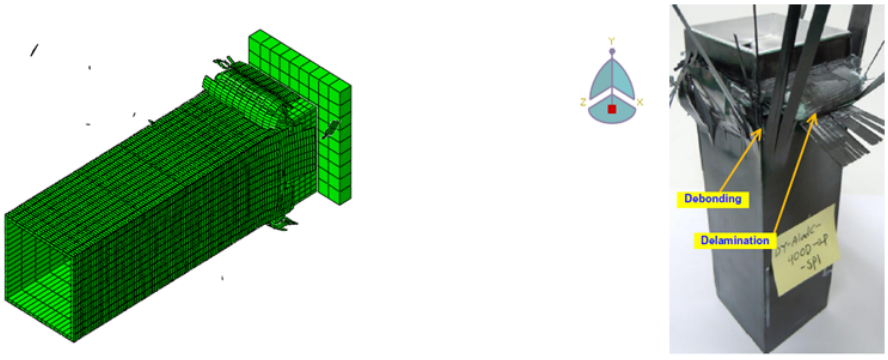

Figure 5.11: Abaqus hybrid beam for [90°/0°] plies. Coarse Mesh

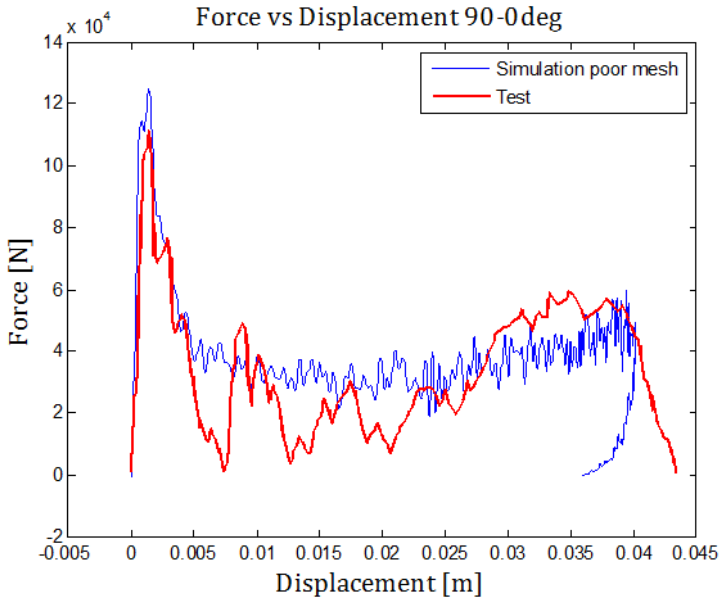

Figure 5.12: Force vs Displacement. Test vs Simulation comparison

The force vs displacement results, 5.12, are very good for this one. Both graphs present almost the same results except for the latter part of the curves when the simulation predicts rebound.

5.3 Results Comparison

Table 5.1: Hybrid beam. Energy absorption depending on ply orientation.

	$0°plies$	$90°/0°plies$	$0°/90°plies$	$+45°/-45°plies$
Coarse Mesh	1.47 KJ	1.58 KJ	1.49 KJ	1.48 KJ
Finer Mesh	1.54 KJ	-	-	-
Test	1.57 KJ	1.48 KJ	1.5 KJ	1.51 KJ

Table 5.2: Hybrid beam. Maximum Displacement (δ_{max}) depending on ply orientation.

	$0°plies$	$90°/0°plies$	$0°/90°plies$	$+45°/-45°plies$
Coarse Mesh	42.7 mm	40.1 mm	35.6 mm	40.4 mm
Finer Mesh	35.4 mm	-	-	-
Test	37.3 mm	43.4 mm	40.8 mm	54.2 mm

For the 0° plies results improve remarkably for the finer mesh as observed in 5.1 and in 5.2. Being the absorbed energy and the displacement much closer to the test's results for the better mesh. The reason why the better mesh was not used for every case was due to the lack of time for doing these computations. Computation's for each of the simple mesh cases would last more than 48h with the use of 8 CPUS. For the finer mesh this time could increase up to 4 or 5 days being unaffordable to perform all the computations for the better mesh.

For 90°/0° orientation, the energy absorbed is quite far but the maximum displacement is close enough.

For the 0°/90° orientation the opposite is true, the results of the absorbed energy are practically the same but the displacement but the displacement predicted in the simulation is quite lower.

Lastly, results of the displacement predicted by the simulation for $+45°/-45°$ are 14mm far from the test's. This is understandable as a different failing mode is occurring for the model.

In spite of the bad results for $+45°/-45°$, the hybrid model is able to predict the displacement sustained and the energy absorbed by the hybrid beam with a small error of about 10% in the worst of the cases. This error could be easily lowered with higher computational power and more time to run the different cases. The model could be then used for designing hybrid structures or to improve the plies orientation finding which one would the the optimum.

CHAPTER 6

CONCLUSIONS, APPLICATIONS AND FUTURE "TO-DO'S"

6.1 Conclusions

Results of the simulations are really good even though many assumptions and simplifications have been taken into account across the project.
The greater simplification is the mesh. The mesh used in the calculations was not optimized. With more time and greater computational power, a refined mesh could have been obtained improving the results. Aluminum properties and composite properties might not be accurate enough. Aluminum plastic data were taken from test data, but there is not information about how it was performed and there is no certainty about the quality of the test. Even if test data were 100% accurate, introducing a non-linear model for the plastic behavior of the Aluminum beam can also add some uncertainty due to the complexity of the approach. Regarding the composite material, its data were taken from a test table. However, for modeling appropriately a composite material this is not enough. The model is not taking into consideration all the complex physical effects occurring in the test. The impact induces elastic waves traveling back and forth trough the structure which combines an isotropic material and an anisotropic one. There is also local buckling of a elastoplastic element. Finally the compression behavior of a brittle anisotropic element is as well a very complex problem. Adding all the above problems which are worked out by Abaqus certainly adds lot of complexity and margin for error to the simulation.

Data from the axial beam crushing test are also missing since it is unknown how the force and the displacement are measured, this may lead to different boundary conditions or arrangement of the parts that could cause a variation of the results.

In spite of all the possible uncertainties, a very complex model has been reproduced with excellent results. With this tool it is possible to predict the local and global behavior of a hybrid beam which can be used to improve the design of these crushing structures, therefore improving the safety of vehicles, airplanes or spaceships which can actually save human lives.

6.2 Applications - Weight Saving of Hybrid Structure.

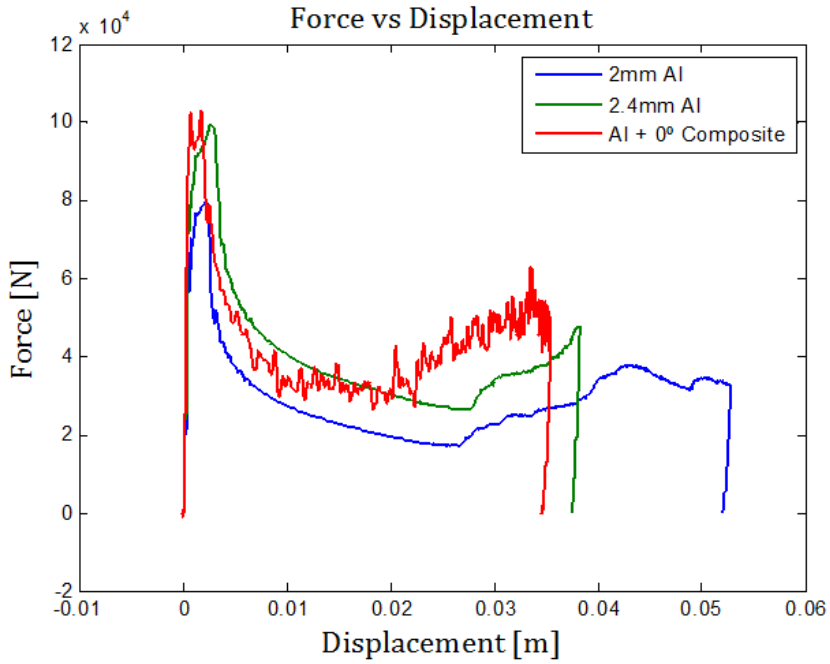

Figure 6.1: Different beam arrangement comparisons

For the best composite orientation, 0° it is then possible to compare how a beam of aluminum of 2.4mm thick would work against the 2mm Aluminum beam reinforced with the composite. It can be seen that for the same thickness, the hybrid beam has better results and furthermore the weight is decreased.

The reduction is not very significant, 20g per beam. However in an industry as demanding as the aerospace in which every gram matters this could actually be a good direction if weight saving is desired.

For a piece of fuselage as the following corresponding to the A320 free fall test:

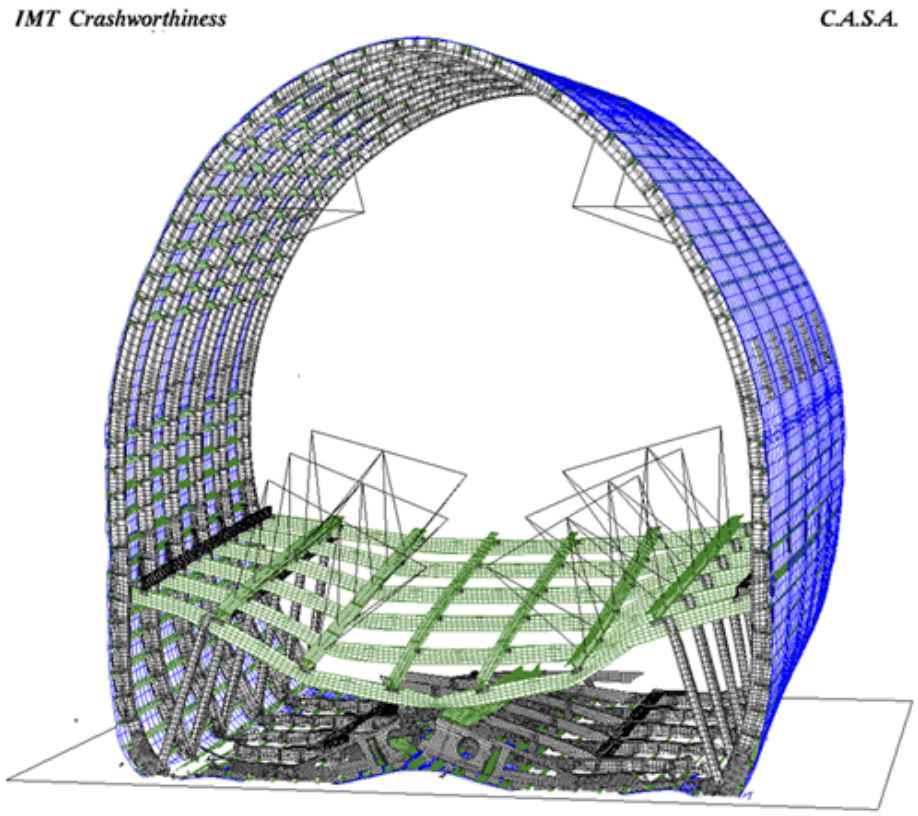

Figure 6.2: A320 fuselage model.Free fall tested

12 beams can be seen in figure 6.2, which would already result in a saving of 240g which is only for a section of the whole fuselage. If we now think about the impact this could have in much greater airplanes such as the A380 (which has 2 floors and its twice as big as the A320) this could mean that 50Kg could be easily saved.

6.3 Future works:

Pam-Crash model was disregarded since the subroutine was not possible to be used for Shell elements. One of the lines of new investigation would be to try and adapt it for shell formulation and include it into Pam-Crash.

It is intended to develop a code which reads the geometry coming from the different softwares and distorts randomly several nodes all along the Aluminum beam to check for mesh distortion theory. It is predicted that in the moment the beam is not perfectly meshed, local buckling will occur as it does in the test and the lobes formation will match the test’s.

Different plies orientations were aimed to be suggested. The lack of computational power made it impossible. For future works it is suggested to try a ply orientation coming from biomimetics. Bones and vegetable are composed by 0° fibers which are the stiffer elements. These plies are surrounded by $+45^\circ$ and -45° plies which constraint out of plane movement of the first plies. Nature has proven to be more than one time above the human race in technology and I do really think it could be interesting to try a stacking sequence bio-based such as $[+45^\circ/-45^\circ/0^\circ/0^\circ/0^\circ/0^\circ/-45^\circ/+45^\circ]$ could present excellent crashing properties. Trying a sequence as complex as that one would carry a huge computational load.

CHAPTER 7

ANNEX - BUDGET

Test

As the work performed is simulation and research there has not been really a pure money or material investment. Nonetheless, the use engineering time and the softwares licensing and CPUS depreciation could be considered in a first approach.

Simulation

Engineering time: 3 $months \cdot 150h/month \cdot 40€/h = 18000€$

Abaqus + Pam-Crash licensing: 2 $(softwares) \cdot 25000€/license.year \cdot 1/4year = 16500€$

Computer Depreciation: This is almost and impossible point to measure. Along the time of the project I have worked my two laptops, one computer at the university and in Airbus I have used up to 36 CPUS at a time.

Total Costs ≈ 25000€

BIBLIOGRAPHY

[1] Zhonghao Bai, Hourui Guo, BinhuiJiang, Feng Zhu,Libo Cao. A study on the mean crushing strength of hexagonal multi-cell thin-walled structures.

[2] Hee Chul Kim,Dong Kil Shin,Jung Ju Lee,Jun Beom Kwon. Crashworthiness of aluminum/CFRP square hollow section beam under axial impact loading for crash box application.

[3] Kim SB, Huh H, Lee GH, Yoo JS, Lee MY. Design of the cross section shape of an aluminum crash box for crashworthiness enhancement of a car. Int J Mod Phys B 2008;22 : 5578 – 83.

[4] W. Abramowicz. Thin-walled structures as impact energy absorbers

[5] Hashin Z. Failure criteria for unidirectional fiber composites, ASME Journal of Applied Mechanics, Vol. 47 (2), 1980, pp 329-334.

[6] G. Allaire and A. Craig: Numerical Analysis and Optimization:An Introduction to Mathematical Modelling and Numerical Simulation.

[7] O. C. Zienkiewicz, R. L. Taylor, J. Z. Zhu : The Finite Element Method: Its Basis and Fundamentals, Butterworth-Heinemann, (2005).

[8] David Roylance.Finite Element Analysis

[9] Abaqus 6.12 Documentation

[10] FM 300 EPOXY FILM ADHESIVE. Cytec Engineered materials datasheet

[11] Progress in the Puck Failure Theory for Fiber Reinforced Composites: Analytical solutions for 3D-stress.Alfred Puck and H. Matthias Deuschle

[12] Out-of-plane failure mechanisms in LFRP composite cutting.C. Santiuste,H. Miguélez,X. Soldani

[13] Prediction of machining induced damage in CFRP composites.Carlos Santiuste, PhD; Álvaro Olmedo, Eng.; Xavier Soldani, PhD; Henar Miguelez, Dr.

[14] Pure Bending Determination of Stress-Strain Curves for an Aluminum Alloy. D. Torres-Franco, G.Urriolagoitia-Sosa, G. Urriolagoitia-Calderón,L. H. Hernández-Gómez, A. Molina-Ballinas, C. Torres-Torres, B. Romero-Ángeles

[15] Wikipedia. Crashworthiness

[16] Wikipedia. Aviation Safety Statistics

[17] The evolution of energy absorption systems for crashworthy helicopter seats. Stanley P. Desjardins

[18] Human Tolerance and Crash Survivability.Dennis F. Shanahan, M.D., M.P.H.